Root niche separation can explain avoidance of seasonal drought stress and vulnerability of overstory trees to extended drought in a mature Amazonian forest

Valeriy Y. Ivanov,[1,2] Lucy R. Hutyra,[3,4] Steven C. Wofsy,[3] J. William Munger,[3] Scott R. Saleska,[5] Raimundo C. de Oliveira Jr.,[6] and Plínio B. de Camargo[7]

Received 8 February 2012; revised 20 October 2012; accepted 31 October 2012; published 11 December 2012.

[1] Large areas of Amazonian evergreen forest experience seasonal droughts extending for three or more months, yet show maximum rates of photosynthesis and evapotranspiration during dry intervals. This apparent resilience is belied by disproportionate mortality of the large trees in manipulations that reduce wet season rainfall, occurring after 2–3 years of treatment. The goal of this study is to characterize the mechanisms that produce these contrasting ecosystem responses. A mechanistic model is developed based on the ecohydrological framework of TIN (Triangulated Irregular Network)-based Real Time Integrated Basin Simulator + Vegetation Generator for Interactive Evolution (tRIBS+VEGGIE). The model is used to test the roles of deep roots and soil capillary flux to provide water to the forest during the dry season. Also examined is the importance of "root niche separation," in which roots of overstory trees extend to depth, where during the dry season they use water stored from wet season precipitation, while roots of understory trees are concentrated in shallow layers that access dry season precipitation directly. Observational data from the Tapajós National Forest, Brazil, were used as meteorological forcing and provided comprehensive observational constraints on the model. Results strongly suggest that deep roots with root niche separation adaptations explain both the observed resilience during seasonal drought and the vulnerability of canopy-dominant trees to extended deficits of wet season rainfall. These mechanisms appear to provide an adaptive strategy that enhances productivity of the largest trees in the face of their disproportionate heat loads and water demand in the dry season. A sensitivity analysis exploring how wet season rainfall affects the stability of the rainforest system is presented.

Citation: Ivanov, V. Y., L. R. Hutyra, S. C. Wofsy, J. W. Munger, S. R. Saleska, R. C. de Oliveira Jr., and P. B. de Camargo (2012), Root niche separation can explain avoidance of seasonal drought stress and vulnerability of overstory trees to extended drought in a mature Amazonian forest, *Water Resour. Res.*, *48*, W12507, doi:10.1029/2012WR011972.

1. Introduction

[2] The role of the Amazon rainforests in the global cycles of carbon, water, and energy is well recognized and has been the subject of numerous studies [e.g., *Salati and Vose*, 1984; *Schlesinger*, 1997; *Davidson et al.*, 2012]. What emerges from much of the research is that the productivity and function of these ecosystems among other factors are profoundly related to climatic variability of precipitation. While the mean annual rainfall over the Amazon basin is ≈ 2100 mm [*Marengo*, 2004], about half of the area [*Sombroek*, 2001; *Xiao et al.*, 2006] experiences a pronounced drought season defined as months with less than 100 mm total precipitation [*Shuttleworth*, 1988]. As demonstrated by *Fatichi et al.* [2012], globally, interannual variability of precipitation is strongly related to precipitation intraannual seasonality; seasonally dry areas of the Amazon are thus statistically likely to experience higher fluctuations of yearly rainfall, as compared to areas with aseasonal rainfall.

[3] Indeed, severe and prolonged droughts in the Amazon have been observed and associated with such climatic variations as the El Ninõ/Southern Oscillation events (warm eastern Pacific) and the anomalously warm tropical Atlantic north-south surface temperature [e.g., *Trenberth and Hoar*, 1997; *Li et al.*, 2006; *Marengo et al.*, 2008].

[1]Department of Civil and Environmental Engineering, University of Michigan, Ann Arbor, Michigan, USA.
[2]Center for the Environment, Harvard University, Cambridge, Massachusetts, USA.
[3]Department of Earth and Planetary Sciences, Harvard University, Cambridge, Massachusetts, USA.
[4]Department of Geography and Environment, Boston University, Boston, Massachusetts, USA.
[5]Department of Ecology and Evolutionary Biology, University of Arizona, Tucson, Arizona, USA.
[6]Brazil Enterprise for Agricultural Research, EMBRAPA Amazonia Oriental, Santarem, Para, Brazil.
[7]Laboratorio de Ecologia Isotopica, University of São Paulo, São Paulo, Brazil.

Corresponding author: V. Y. Ivanov, Department of Civil and Environmental Engineering, University of Michigan, 1351 Beal Ave., 105 EWRE, Ann Arbor, MI 48109, USA. (ivanov@umich.edu)

0043-1397/12/2012WR011972

The frequency and severity of droughts may change in the future, and some global circulation models project drying of the region over the 21st century [*Trenberth and Hoar*, 1997; *Harris et al.*, 2008; *Salazar et al.*, 2007; *Malhi et al.*, 2008]. This may be further exacerbated by ecosystem feedbacks, such as reduced transpiration from the forests [*Huntingford et al.*, 2008], decreasing the current 25%–50% recycling of regional rainfall [*Eltahir and Bras*, 1994], and the processes of deforestation [*Nobre et al.*, 1991; *Costa and Foley*, 2000; *Werth and Avissar*, 2002; *Oyama and Nobre*, 2003].

[4] The pronounced rainy and dry seasons, particularly in the central and eastern Amazon Basin [e.g., *Sombroek*, 2001; *Malhi and Wright*, 2004; *Xiao et al.*, 2006], have significant implications for the system function [*Brando et al.*, 2010; *Davidson et al.*, 2012]. It is a matter of significant scientific concern to identify to what degree the Amazon rainforests are vulnerable to droughts. As recent research indicates, the understanding of drought effects and essential controlling factors of the rainforest function are yet to be fully understood.

[5] Specifically, remote sensing [e.g., *Huete et al.*, 2006; *Myneni et al.*, 2007; *Saleska et al.*, 2007] and ground-based observations [e.g., *Saleska et al.*, 2003; *Goulden et al.*, 2004; *da Rocha et al.*, 2004; *Hutyra et al.*, 2007; *Hasler and Avissar*, 2007] indicate higher photosynthetic activity and increased CO_2 uptake and water fluxes during the dry season than in the wet season. One logical inference is that the rainforest is at least in part light-limited, not water-limited, and thus reduced cloud cover and increased incoming radiation during the dry seasons favorably affect forest productivity, resulting in higher transpiration fluxes [*Hutyra et al.*, 2007; *Nemani et al.*, 2003]. Early modeling studies, however, often predicted an opposite pattern of ecosystem dynamics. In a typical model simulation reproducing dry season conditions, available water was quickly depleted through evapotranspiration and/or recharge of deep aquifers, and water stress would set in long before the end of drought conditions. Overall, vegetation activity was suppressed in these model simulations, which could not reproduce the persistence of transpiration fluxes throughout the entire dry season [e.g., *Saleska et al.*, 2003; *Werth and Avissar*, 2004; *Lee et al.*, 2005].

[6] Various hypotheses have been proposed to explain the extremely high drought tolerance of the rainforest, including (1) deeply penetrating root systems [*Nepstad et al.*, 1994; *Jipp et al.*, 1998; *Baker et al.*, 2008; *Grant et al.*, 2009; *Markewitz et al.*, 2010], (2) the phenomenon of "hydraulic redistribution" [e.g., *de Oliveira et al.*, 2005; *Lee et al.*, 2005; *Baker et al.*, 2008], (3) uptake of water directly by leaves during dry season rains and nighttime dew events [*Cardinot*, 2008], and, more recently, (4) the regional effects of a high water table [*Fan and Miguez-Macho*, 2010].

[7] The evidence available to support or contradict each of these hypotheses is variable. First, in the case of maximum rooting depth, the presence of roots at depths > 10 m is clear, but their function remains quite uncertain, and their importance cannot be confirmed or denied as yet. The open questions are how deeply roots can really grow, what kind of hydraulic limitations exist on the transfer of water from deep locations to the top of canopy, and whether there are sufficient roots at deep locations. For example, *Nepstad et al.* [1994] estimated that only about 10% of the total rooting mass of a forest was at depths between 4 and 10 m. In a modeling study, *Grant et al.* [2009] demonstrated that a root system depth of only 8 m was needed to avoid water limitations for a 5-month dry season, but the generality of such an inference remains uncertain. Second, the phenomenon of hydraulic redistribution (i.e., the process of water transfer by roots following the countergradient of soil water potential, most efficient when transpiration uptake is negligible) has been well documented for arid and temperate climate plant species (e.g., for a review see *Caldwell et al.* [1998]) and has been demonstrated for three tree species in the Tapajós National Forest, Brazil [*de Oliveira et al.*, 2005]. One may note that *de Oliveira et al.* [2005] observed sap flow reversals; whether this is a sufficiently strong argument for advocating the importance of hydraulic redistribution for the entire ecosystem function [e.g., *Lee et al.*, 2005] remains uncertain. Other field and modeling experiments postulate that, in fact, the mechanism of hydraulic redistribution cannot contribute significantly to the soil water dynamics [e.g., *Romero-Saltos et al.*, 2005; *Markewitz et al.*, 2010]. A conclusion is that further empirical evidence is needed to assess whether hydrologically significant amounts of water can be transferred and deposited in soil-surrounding roots. So far, quantitative assessments for the Amazon region come from modeling studies that yield estimates "on the upper end of the spectrum" [e.g., *Neumann and Cardon*, 2012], as compared to most laboratory and in situ measurements. Third, a similar comment concerns the mechanism of water uptake by leaves: further, quantitative empirical evidence is needed to confirm the plausibility of its significance. Lastly, a recent claim of possibly predominant groundwater effects [*Fan and Miguez-Macho*, 2010] cannot be supported by field observations at some of the "benchmark" sites [e.g., *Goulden et al.*, 2004; *Hutyra et al.*, 2007; *Nepstad et al.*, 2002]: They present no evidence of shallow water table. The question of the exact water-stress avoidance mechanism has therefore not been fully resolved. Other explanations should be attempted that will help focus future observational campaigns, so that "unfit hypotheses" [*Popper*, 1972] can be objectively evaluated.

[8] This study makes a further effort to study the hydrology of an Amazonian rainforest. A vegetation-hydrology model that parameterizes the essential canopy-soil water-energy processes using a simplified three-big-leaf representation of canopy vertical structure is developed. The representation of a very deep ($\sim$36 m) soil profile allows the model to explicitly resolve the propagation of wetting and drying cycles into the soil column underlying forest vegetation. Comprehensive observational data from a flux tower site in Tapajós National Forest, Brazil, are used in this study. Meteorological data from the tower for the period of 2002–2005 serve as the model forcing. Observed canopy phenology, energy fluxes, soil texture and water retention properties, and profiles of root biomass are used to parameterize and constrain the model performance. A set of numerical experiments has been designed to address (1) depth of the rainforest root system as the only strategy for stress avoidance; (2) the capillary properties of clayey Oxisol soils that could possibly lead to the upward flow of water from soil layers below the deepest extent of roots; specifically, if a sufficiently high gradient of soil matric potential is created in the root zone because of moisture uptake by plants, a flow in the

direction opposite to the gravitational force may take place; and (3) the existence of specific water uptake niches in the soil column (i.e., substantially different depths of centroids of moisture uptake profiles) corresponding to root systems of trees located at different levels in the vertically structured canopy, i.e., overstory, midsize, and understory trees. These several possible explanations of the water-stress avoidance paradigm either have not been considered in sufficient detail in models or have remained entirely unexamined. Neither hydraulic redistribution nor leaf water uptake is addressed in this model application, and the role of groundwater is eliminated by the choice of site (see section 2.1).

[9] One of the indirect facts pointing to the plausibility of the hypothesis referring to the existence of water uptake niches is the remarkable agreement of the main outcomes of two long-term rainfall exclusion experiments described by *Nepstad et al.* [2002, 2007] and *da Costa et al.* [2010] as well as a pan-tropical assessment of drought-related tree mortality by *Phillips et al.* [2010], and, to some extent, observations for a neotropical forest system by *Condit et al.* [1995]: in all studies, there was an asymmetric response to prolonged droughts by overstory and understory trees. Specifically, large trees were consistently found to be the most vulnerable. Synthetic numerical experiments augmenting this study mimic the drying signal of rainfall exclusion experiments and consistently with empirical observations reproduce an asymmetric response by large and small trees in conditions of root niche separation. A subsequent analysis demonstrates a relative sensitivity of study inferences with respect to the key parameters quantifying plant water limitations. Overall, this study is best described as a model-based analysis of the plausibility of various mechanisms, attempting to address a wide spectrum of empirical observations.

2. Data and Methods

2.1. Site Description

[10] Data are from the flux tower site in Tapajós National Forest (Brazil) (2°51.4′S, 54°57.5′W) near km 67 (referred to as "km 67" throughout) of the Santarém-Cuiabá highway BR-l63. The site was a part of the large-scale biosphere-atmosphere experiment in Amazonia (LBA-ECO) and has been used in a number of studies described in previous publications [e.g., *Hutyra et al.*, 2007; *Rice et al.*, 2004; *Vieira et al.*, 2004; *Saleska et al.*, 2003]. Additionally, a large throughfall exclusion experiment was established in the relative proximity of the flux tower (∼5 km) in 2000 [*Nepstad et al.*, 2002], which monitored a variety of ecosystem characteristics in the l-ha treatment and control plots [e.g., *Brando et al.*, 2008; *Nepstad et al.*, 2007]. These studies provide a complete description of different system characteristics, and the reader is referred to the cited papers for details. The region has a mean annual temperature of 25°C with a mean annual precipitation of ∼2000 mm, variable between 600 and 3000 mm yr^{-1} [*Nepstad et al.*, 2002]. The area is subjected to a seasonal drought, i.e., months with less than 100 mm precipitation, with a mean span of 5 months, typically lasting from 15 July to 15 December [*Parrota et al.*, 1995]. The water table is very deep, ∼100 m below the soil surface [*Nepstad et al.*, 2002]. Soils are clay-rich, deeply weathered Oxisols. Patches of higher sand content (Santarém Ultisols) occur on slopes and in topographic lows of the surrounding area but not at the study site. The forest is located on flat terrain, an erosional remnant plateau, with a limited drainage network formed on sediments of the Barreiras formation [*Silver et al.*, 2000]. The forest has a closed canopy with a mean height of approximately 40–45 m and emergent trees reaching up to 55 m. The vertical canopy distribution is stratified [*Vieira et al.*, 2004] with a fairly distinct three-level structure that represent the highest, midrange, and smallest trees. The forest at the site exhibits a robust increase of latent heat flux during dry seasons (for details, see *Hutyra et al.* [2007]), responding to increased light levels (Figure S1a in the auxiliary material).[1] The annual variation of foliage leaf area index (LAI) is within 10% of the maximum value, with the maximum apparently out of phase with the radiation cycle (Figure S1b in the auxiliary material and *Brando et al.* [2010]). *Domingues et al.* [2005] showed that the leaf density was approximately constant throughout the canopy profile, with about 35% of leaf area attributed to the top 10 m of the canopy.

2.2. Hydrometeorological Forcing Data

[11] Gap-filled meteorological data for the period of January 2002 to January 2006 are used as atmospheric forcing to the model. Specifically, the hourly time series of the following variables observed at km 67 [*Hutyra et al.*, 2007] serve as the model input: hourly precipitation (measured at 42.6 m above the forest floor), air temperature (57.8 m), water vapor partial pressure (computed from vapor molar concentration measured at 62.2 m), wind speed (57.8 m), CO_2 partial pressure (measured as molar concentration at 62.2 m), atmospheric pressure (ground level), and incoming short-wave and long-wave radiation fluxes. Data gaps were fairly insignificant (1%–9% of the series) for most of the variables and were filled with the mean monthly values corresponding to the hour of the day with the missing value. Only radiation data contained a large fraction of gaps (∼35%–55% of the series), and thus several sources/methods were used to complete the series. The gap-filling procedure is outlined in the auxiliary material (section S.1).

2.3. Soil Hydraulic Properties

[12] The soils at the km 67 site study are clayey Oxisols that are deeply weathered with no concretions or impeding layers, at least in the upper 12 m [*Nepstad et al.*, 2007]. The van Genuchten-Mualem soil hydraulic model [*van Genuchten*, 1980] was chosen to describe the dependence of conductivity and soil matric pressure on moisture content. Due to the absence of detailed, on-site measurements of soil hydraulic properties as well as uncertainty associated with each indirect method, several approaches and data sources were used to infer the saturated conductivity and soil water retention parameters. Previously reported soil water retention parameters by *Belk et al.* [2007] did not favorably compare with the other independently obtained parameterizations (see sections 2.3.2–2.3.4 and Figure 1) and therefore were not used. Note that the generated

[1] Auxiliary materials are available in the HTML. doi:10.1029/2012WR011972.

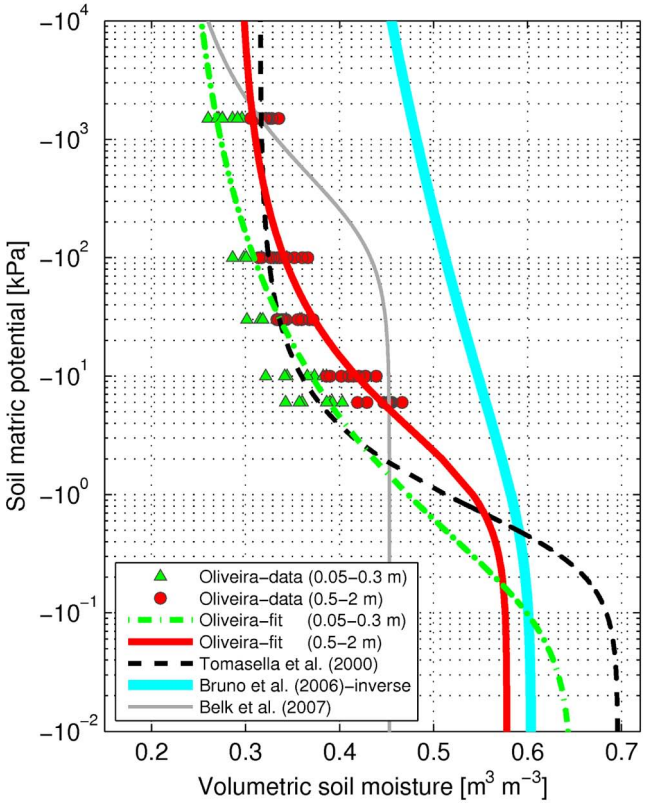

Figure 1. Soil water retention data and curves obtained in this study. The curves were parameterized according to the van Genuchten-Mualem soil hydraulic model [*van Genuchten*, 1980]. The legend notation refers to the following sources: "Oliveira-data" refers to the data obtained from R. C. de Oliveira Jr. in 2007; "Oliveira-fit" refers to the fit curves obtained for the former data for different depth ranges; "Tomasella et al. (2000)" refers to parameters obtained with the pedotransfer functions of *Tomasella et al.* [2000] using field soil texture data of L. Hutyra (obtained in 2003); "Bruno et al. (2006)-inverse" refers to the parameters of soil water retention curve obtained using an inverse procedure of *Hou and Rubin* [2005]; and "Belk et al. (2007)" refers to the curve obtained by geometric averaging of depth-interpolated parameters reported by *Belk et al.* [2007].

ensemble of soil parameterizations permits addressing robustness of study inferences with respect to uncertain properties of the soil. Following sections describe the methodology used in obtaining the parameter values.

2.3.1. Saturated Hydraulic Conductivity

[13] Values of the saturated hydraulic conductivity were digitized from the manuscript of *Belk et al.* [2007], who measured conductivity over the upper 4 m of the soil profile. Geometric averaging of depth-interpolated values was carried out to obtain $K_{sn} = 35.6$ mm h^{-1} for the 0.05–0.3 m depth range and $K_{sn} = 14.1$ mm h^{-1} for the 0.3–4.0 m depth range. These values were used in the two scenarios described in sections 2.3.2 and 2.3.3.

2.3.2. Measured Soil Water Retention Data

[14] The soil water retention data were obtained by the authors in 2007 (unpublished data set). Soil samples were collected at a location that is in relative proximity to km 67 (within ~1 km radius); however, the exact location was not recorded. Laboratory measurements of water retention properties were carried out for the following soil matric pressures: 6, 10, 33, 100, and 1500 kPa. Samples were taken from the following depths: 5, 15, 30, 50, 100, and 200 cm. Due to significant differences in the soil water retention data between the surface layer and deeper layers, the measurements were grouped according to the following depth ranges: 0.05–0.3 m (what is referred to as "CO-surface" group) and 0.5–2 m ("CO-deep" group). These two sets of parameters define the "CO" soil hydraulic parameterization. A nonlinear optimization of parameter values of the *van Genuchten* [1980] model was subsequently carried out. The data and the fitted water retention curves for the two depth ranges are shown in Figure 1. The corresponding parameter values are provided in Table 1.

2.3.3. Parameter Estimation Using Pedotransfer Functions

[15] *Tomasella et al.* [2000] developed generic pedotransfer functions for South American soils, allowing one to derive the parameter values of the *van Genuchten* [1980] model based on soil textural and chemical composition. Field soil texture data were obtained by the authors in 2003 (unpublished data set): the surface soil (top 10 cm) composition was reported as 91% clay, 7.8% silt, and 1.2% sand. The organic carbon content was reported as 2.68 g kg^{-1}, and soil bulk density was measured as 1.0225 g cm^{-3}. As the fraction of sand that was fine was unknown, it was assumed to be either 0%, 50%, or 100%. Using the *Tomasella et al.* [2000] functions, three parameter sets were estimated assuming these fractions. The obtained parameter sets differed only slightly, and thus they were geometrically averaged to obtain a single parameter set. The derived water retention curve representative of the entire soil column is shown by the Tomasella et al. (2000) curve in Figure 1.

Table 1. Soil Hydraulic[a], Heat Transfer and Albedo[b] Parameters for Different Soil Parameterization Scenarios

Soil Scenario[c]/Parameter	K_{sn}	θ_s	θ_r	n	α
CO-surface[c]	35.6	0.647	0.225	1.237	−0.0883
CO-deep[c]	14.1	0.578	0.291	1.413	−0.00674
TH[c]	14.1	0.696	0.315	1.687	−0.0224
MRE[c]	26.9	0.604	0.283	1.0623	−0.0213

[a] K_{sn} (mm h^{-1}) is the saturated hydraulic conductivity in the normal to the soil's surface direction, θ_s (m^3 m^{-3}) is the saturation moisture content, θ_r (m^3 m^{-3}) is the residual moisture content, n and α (mm^{-1}) are the fit parameters of the van Genuchten-Mualem soil hydraulic model [*van Genuchten*, 1980]. The soil albedo and heat transfer parameters are assumed to be uniform for all soil parameterizations.

[b] Since undercanopy soil is assumed to be a Lambertian surface, albedos for direct beam, α^{μ}_{Λ}, and diffuse, α_{Λ}, shortwave radiation fluxes are equal. The values of the shortwave albedos for saturated soil ($\alpha^{\mu}_{\mathrm{sat}\,\Lambda} = \alpha_{\mathrm{sat}\,\Lambda}$) are 0.11 for the visible and 0.225 for the near-infrared spectral bands, respectively [*Ivanov et al.*, 2008]. The values of the shortwave albedos for *dry* soil ($\alpha^{\mu}_{\mathrm{dry}\,\Lambda} = \alpha_{\mathrm{dry}\,\Lambda}$) are 0.22 for the visible and 0.45 for the near-infrared spectral bands, respectively. The soil heat transfer properties are assigned the following values: $k_{s,\mathrm{dry}} = 0.4$ and $k_{s,\mathrm{sat}} = 3.3$ J m^{-1} s^{-1} K^{-1} are the dry and saturated soil thermal conductivities, respectively, and $C_{s,\mathrm{soi}} = 1.5 \times 10^6$ J m^{-3} K^{-1} is the heat capacity of the soil solid [*Ivanov et al.*, 2008].

[c] See section 2.3 for the definitions of soil parameterization scenarios.

The corresponding parameter values are provided in Table 1 as the "TH" parameterization.

2.3.4. Inverse Parameter Estimation

[16] An inverse method of *Hou and Rubin* [2005] was used to derive soil properties using soil water dynamics data resolved at multiple depths. The only available high-frequency, long-term record of soil moisture data was available for a site at km 83 of the Santarém-Cuiabá highway [*Bruno et al.*, 2006]. This data set was used in the inverse estimation procedure. Eight cases were selected corresponding to 10–11 h nighttime intervals with zero or insignificant observed evaporation. The cases included periods with the highest and lowest observed soil moisture, as well as the cases with the highest moisture variability in the 10 m soil profile. Several attempts to derive layer differences yielded posterior distributions that were identical to prior distributions. Therefore, the final search aimed to estimate hydraulic properties representative of the entire soil column. The derived water retention curve is shown in Figure 1. The depth-uniform saturated hydraulic conductivity was estimated to be $K_{sn} = 26.9$ mm h^{-1}. The corresponding parameter values are provided in Table 1 as the "MRE" parameterization.

2.4. Root Profiles

[17] Data on the distributions of root biomass density were obtained as one of the outcomes of the throughfall exclusion experiment [*Nepstad et al.*, 2002] that was carried out in the relative proximity of the flux tower (~5 km). For the treatment site, only data obtained before the beginning of the experiment were used. Observations of fine root biomass were used (a fine root has the diameter smaller than 2 mm) assuming the suberized fraction of a fine root is small and almost the entire root surface can be used for plant moisture uptake [*Taiz and Zeiger*, 2006, p. 56]. Fine root distributions were therefore associated with uptake profiles. A "generalized" root profile was created based on the actual measurement data shown in Figure 2a. Two

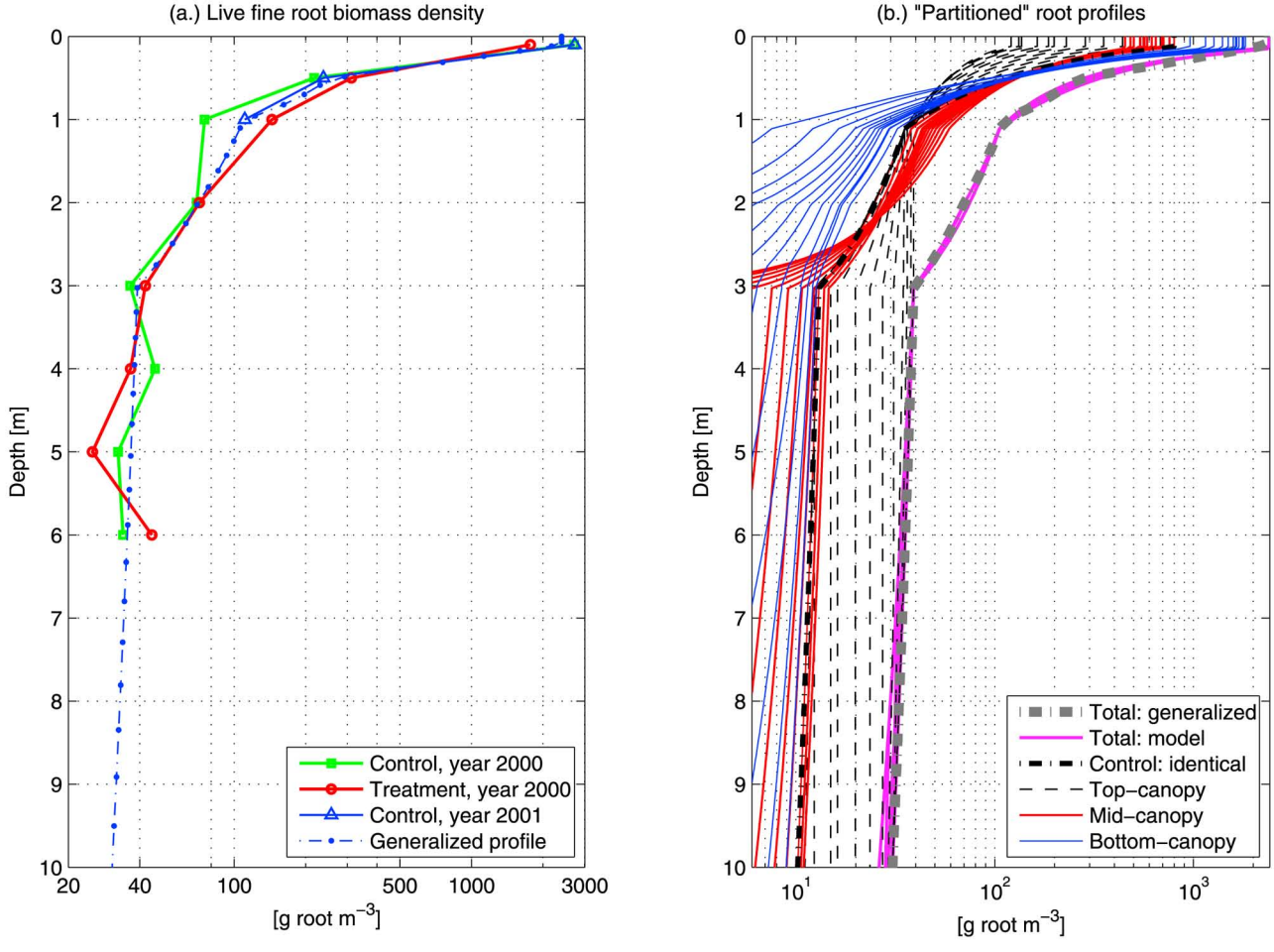

Figure 2. Profiles of root biomass distribution: (a) Live fine root density from *Nepstad et al.* [2002], corresponding to measurements in the "control" and "treatment" plots, and a generalized profile obtained in this study and (b) hypothesized root profiles (section 2.5.4) obtained by partitioning the observed profile of bulk root biomass into profiles corresponding to top-, mid-, and bottom-canopy trees. In total, 13 different permutations of root profiles were generated. The "Total: generalized" represents the generalized profile of bulk root density shown in Figure 2a; the "Total: model" profiles are obtained by summing three density profiles corresponding to different trees (13 permutations). The "Control: Identical" profile illustrates the control root scenario, i.e., all tree types have the same root density profile.

scenarios of maximum root depth were considered: $Z_{\mathrm{RootS}} = 6$ m and $Z_{\mathrm{RootD}} = 30.2$ m. The procedure resulting in these magnitudes is described in the auxiliary material, section S.2. The corresponding root profiles were used in the modeling efforts (section 2.5.4).

2.5. Modeling Efforts

[18] An ecohydrological model that parameterizes essential canopy-soil water-energy processes using a three-big-leaf representation of canopy vertical structure and a finely resolved deep soil profile was developed in this study. As is the case with any modeling effort, a number of simplifying assumptions were made in the representation of structural elements of the vegetation-hydrology system, its intra- and interannual dynamics, as well as in the description of relevant physical processes. These are outlined in the following.

2.5.1. Ecohydrological Model

[19] An ecohydrologic model [*Ivanov et al.*, 2008], TIN (Triangulated Irregular Network)-based Real Time Integrated Basin Simulator + Vegetation Generator for Interactive Evolution (tRIBS+VEGGIE), is used in this study. The model mimics principal water and energy processes over the complex topography of a river basin and links them to essential plant biochemical processes and phenology. The model design emphasizes dynamic interactions between vegetation system and subsurface hydrological dynamics. Each computational element exhibits a "big-leaf" representation of the canopy coupled to a multilayer soil-root model that computes soil moisture and heat transport and root water uptake.

[20] Because topography within the tower footprint is flat (section 2.1) and relevant observations on canopy dynamics (section 2.5.3) were available, the model application was "reduced." Specifically, the model was applied at the plot scale, and vegetation dynamics were not explicitly simulated. Only the biochemical model of canopy stomatal behavior [*Farquhar et al.*, 1980; *Collatz et al.*, 1991] was used to simulate the response of latent heat flux to the ambient environment. The amount of leaf area as well as structural characteristics of vegetation were imposed as a predetermined model input (see section 2.5.3). Furthermore, the model formulation described in *Ivanov et al.* [2008] has been substantially modified to adapt the model to conditions of the study site that exhibits complex canopy structure and deep soils. These changes are briefly outlined in the auxiliary material, sections S.3 and S.4. For the reader's convenience, Appendix A provides the formulation of a heuristic soil moisture availability factor, β_T, which is frequently used throughout the text. In short, the formulation of the lumped factor $\beta_T \in [0, 1]$ is based on widely used relationships [*Bonan*, 1996; *Feddes et al.*, 2001] that parameterize a decrease of water availability with drying soil conditions. The factor is used to regulate the stomatal conductance when transpiration flux is computed and its departure from unity indicates soil control on the flux; $(1 - \beta_T)$ can be interpreted as a metric of water stress. Table 2 contains the parameter values used in this study. The notation used for the parameters is the same as that of *Ivanov et al.* [2008].

2.5.2. Soil Profile

[21] In representing the soil profile in the model, two conditions had to be accounted for: (1) the capability to incorporate the deepest root profile with $Z_{\mathrm{RootD}} = 30.2$ m and (2) the need of providing a sufficient soil buffer under the root zone to alleviate the effect of an assumed free drainage boundary condition at the bottom of the soil column. With respect to the latter, the intention was to create a soil buffer that could generate upward unsaturated flow if sufficiently high tensions developed in the root zone because of moisture uptake by roots. Consequently, a deep, 36 m soil profile was used to model the subsurface soil moisture dynamics. A regular mesh resolution was selected to be 30 mm, which resulted in 1200 computational nodes.

Table 2. Vegetation Biophysical, Photosynthesis, Interception, and Water Uptake Parameters Used in the Model[a]

Parameter/Canopy Level[b]	Top-Canopy	Mid-Canopy	Bottom-Canopy
Biophysical Parameters			
d_{leaf}	0.05	0.05	0.05
χ_L	0.10	0.10	0.10
$\alpha_\Lambda^{\mathrm{leaf}}$ -VIS	0.11	0.05	0.02
$\alpha_\Lambda^{\mathrm{leaf}}$ -NIR	0.50	0.50	0.50
$\alpha_\Lambda^{\mathrm{stem}}$ -VIS	0.20	0.20	0.20
$\alpha_\Lambda^{\mathrm{stem}}$ -NIR	0.45	0.45	0.45
$\tau_\Lambda^{\mathrm{leaf}}$ -VIS	0.07	0.02	0.01
$\tau_\Lambda^{\mathrm{leaf}}$ -NIR	0.33	0.32	0.32
$\tau_\Lambda^{\mathrm{stem}}$ -VIS	0.0001	0.0001	0.0001
$\tau_\Lambda^{\mathrm{stem}}$ -NIR	0.0001	0.0001	0.0001
Photosynthesis Parameters			
$V_{\mathrm{max}\ 25}$	40.0	35.0	30.0
$\overline{K}$	0.35	0.35	0.35
m	9	9	9
b	10,000	10,000	10,000
$\epsilon_{3,4}$	0.055	0.06	0.065
Interception Parameters			
K_c	0.15	0.15	0.15
g_c	3.7	3.7	3.7
Water Uptake Parameters			
Ψ^*	−0.50	−0.50	−0.50
Ψ_w	−2.50	−2.50	−2.50

[a] For Details, see *Ivanov et al.* [2008].

[b] d_{leaf} (m) is the mean leaf size; χ_L is the parameter of departure of leaf angles from a random distribution; $\alpha_\Lambda^{\mathrm{leaf}}$ and $\tau_\Lambda^{\mathrm{leaf}}$ (−) are the leaf reflectances and transmittances, respectively; $\alpha_\Lambda^{\mathrm{stem}}$ and $\tau_\Lambda^{\mathrm{stem}}$ (−) are the stem reflectances and transmittances, respectively; "VIS" and "NIR" are used to denote the visible and near-infrared spectral bands, respectively; $V_{\mathrm{max}\,25}$ (μmol CO_2 m^{-2} s^{-1}) is the maximum catalytic capacity of Rubisco at 25°C; $\overline{K}$ (−) is the time-mean photosynthetically active radiation (PAR) extinction coefficient used to parameterize a decay of nitrogen content in the canopy; m (−) is an empirical parameter used as a slope factor in a linear model relating the net assimilation rate and stomatal conductance; b (μmol m^{-2} s^{-1}) is the minimum stomatal conductance; $\epsilon_{3,4}$ (μmol CO_2 μmol^{-1} photons) is the intrinsic quantum efficiency of CO_2 uptake; K_c (mm h^{-1}) is the canopy water drainage rate coefficient; g_c (mm^{-1}) is the exponent parameter of canopy water drainage rate; Ψ^* (MPa) is the soil water potential at which stomatal closure begins; and Ψ_w (MPa) is the soil water potential at which plant wilting begins.

2.5.3. Above-Ground Vegetation Components

[22] A three-big-leaf representation of the forest canopy was developed in an attempt to represent the vertical structure of the canopy, which has been observed to be distinctly stratified [*Vieira et al.*, 2004]. *Rice et al.* [2004] describe "emergent," "canopy," "subcanopy," and "suppressed" trees. In this study, the "top-canopy" (overstory) trees represent the emergent and canopy trees; the "mid-canopy" and

"bottom-canopy" (understory) trees, respectively, represent subcanopy and suppressed trees. These types of trees were assumed to be sufficiently different in their biophysical and biochemical properties, for example, reflecting observed changes in the characteristics of sunlit and shaded plants [e.g., *Taiz and Zeiger*, 2006]. The outcome of such an assumption is that different canopy levels represented different tree functional types, even though some of the same species are likely to be present in each canopy level. Note the interchangeable use of "tree type" and "canopy layer" in the following text. Details of treatment of canopy layers are presented in the auxiliary material, section S.3; the parameter values are provided in Table 2.

[23] The amount of leaf area as well as structural characteristics of vegetation were imposed as predetermined model input. The data on canopy dynamics were obtained from the database of the LBA experiment in Amazonia (http://lba.cptec.inpe.br). This data set contains measurements of total LAI obtained at monthly intervals in the control plots of the rainfall exclusion experiment [*Nepstad et al.*, 2002]. The LAI data span the period of 2000–2004. According to *Domingues et al.* [2005], the leaf density is approximately constant throughout the canopy profile at the site; consequently, the mean annual cycle of LAI for each of the "big leaves" was obtained by dividing the total LAI (auxiliary material, Figure S1b) by three.

[24] The stem area index (SAI) [e.g., *Bonan*, 1996] was assumed to be 0.2 [$m^2\ m^{-2}$ ground area] for each of the tree types. Each canopy layer was assumed to be uniformly occupying the entire plot area, i.e., the vegetation fraction was set to one for each of the tree types. This apparent simplification neglects the spatial heterogeneity of the canopy, i.e., the existence of gaps as well as patches with LAI higher than the one assumed. Remote-sensing data that permit the inverse estimation of LAI, e.g., the data from moderate resolution imaging spectroradiometer (MODIS; http://modis.gsfc.nasa.gov, *Myneni et al.* [2002]), do not offer sufficient resolution and quality to assess the degree of such variability at the study site. The importance of representation of canopy heterogeneity at the tree scale is hard to assess since relevant studies are still in their nascence [e.g., *Bohrer et al.*, 2009].

2.5.4. Below-Ground Vegetation Components

[25] Each of the tree types defined above according to the canopy level (section 2.5.3) contributes to the distribution of fine root biomass described in section 2.4. A first-order assumption one can make is that each of the types contributes equally to the observed density at any depth z and therefore root density for any tree type can be obtained as the total root biomass divided by three. For each of the considered maximum root depths, Z_{RootD} and Z_{RootS}, this serves as the "control" scenario (Figure 2b) against which all other root distribution scenarios are compared.

[26] Certainly, the control root distribution case is only one plausible scenario of the shape of individual profiles corresponding to trees that have different positions in the canopy. Because it is practically impossible to quantify the distribution of root biomass of a given tree type in the bulk root biomass from in situ observations (and to the author's knowledge, there are no available generic methodologies), this study has generated an ensemble of individual root distributions. The developed ad hoc partition procedure (see the auxiliary material, section S.5) yielded 12 additional permutations of individual root profiles that are illustrated in Figure 2b for the maximum root depth Z_{RootD}. As the number of permutation scenario increases from 1 (the control) to 13, the profiles become more different from the control root scenario and trees of the upper-canopy level contain progressively higher fraction of roots at deeper locations (Table 3), while trees of the bottom-canopy layer contain higher fraction of roots at shallower soil layers. Note that this also implies varying root depths for all scenarios other than the control one. For example, as Table 3 illustrates, in the case of the largest difference among the profiles, i.e., the root scenario 13 referred to thereafter as the "scenario with distinct niches," the roots of understory trees extend only to ~2.01 m, the root depth of mid-canopy trees is ~3.03 m, while the roots of overstory trees occupy the entire depth Z_{RootD} (30.2 m).

[27] The depth $Z_{RootS} = 6$ m was considered in the design to represent another choice of the maximum possible root depth. Thirteen root permutations were generated by terminating the individual profiles shown in Figure 2b at Z_{RootS} to exclude roots beyond that depth. Similar to the scenarios

Table 3. An Illustration of Hypothesized Root Fractions Contained in Different Soil Layers for Trees Occupying Particular Canopy Levels[a]

Root Scenario/Metric	Root Fraction 0–30 cm (%)	Root Fraction 30–60 cm (%)	Root Fraction 60–100 cm (%)	Root Fraction 100 cm - Root Depth (%)	Root Depth (cm)
Z_{RootS}: control scenario					
Top-, mid-, bottom-canopy	54.7	12.3	6.8	26.2	600
Z_{RootS}: distinct niches scenario					
Top-canopy	12.5	7.1	6.9	73.5	600
Mid-canopy	46.2	17.0	12.5	24.3	303
Bottom-canopy	88.2	8.8	2.2	0.8	201
Z_{RootD}: control scenario					
Top-, mid-, bottom-canopy	36.5	8.2	4.6	50.7	3020
Z_{RootD}: distinct niches scenario					
Top-canopy	4.27	2.43	2.40	90.9	3020
Mid-canopy	46.2	17.0	12.5	24.3	303
Bottom-canopy	88.2	8.8	2.2	0.8	201

[a]Two maximum root depths, Z_{RootS} and Z_{RootD}, are used. Note that the values reported were obtained in relation to the total hypothesized biomass within the root depth (last column of the table), i.e., a small fraction for a deep root zone can imply a large absolute surface area. The actual spatial resolution of the subsurface model is 30 mm; the values shown were obtained by lumping root fractions for specified soil layers.

for Z_{RootD}, scenario 1 among these permutations represents the control and scenario 13 corresponds to the scenario with distinct niches (Table 3).

[28] Overall, 26 root scenarios (the control scenario plus 12 permutations of individual root profiles for the two maximum root depths Z_{RootD} and Z_{RootS}) for each soil type were generated. In total, this resulted in 78 simulation scenarios.

[29] The ecohydrology model requires the input of a potential strength of moisture sink in each subsurface mesh node [*Ivanov et al.*, 2008]. Such a profile is obtained by computing the fraction of roots contained in a control volume of each mesh node with respect to the total root biomass.

2.5.5. Soil Moisture Initialization

[30] The deep soil profile of a fine-textured soil may exhibit significant memory effects due to the persistence of soil moisture initial conditions in simulations. This study attempted to minimize such adverse initialization impacts by using a model "spin-up." Specifically, each scenario of maximum root depth (Z_{Root}) for each soil type was simulated with 20 years of meteorological forcing obtained as five 4-year cycles of the original forcing data, January 2002 to January 2006. The soil matric head profile at the end of each of these spin-up simulations was used to initialize simulations for the corresponding combination of soil type and root depth.

3. Results

3.1. Model Calibration

[31] The tRIBS+VEGGIE model does not have an automated parameter calibration routine. Manual model calibration was carried out with the main objective to match the observed daily and seasonal cycles of net radiation, latent and sensible heat fluxes.

[32] Because the study addresses the effects of dry periods on vegetation water uptake, the soil hydraulic parameters (Table 1) and the root fractions specifying the strength of transpiration moisture sinks (see Appendix A, equation (A2)) should also be considered as unknown parameters. An arbitrary choice of soil type and root distribution would be unjustified because both can strongly affect the dynamics of plant water limitations. Therefore, the calibration strategy was based on the assumption that forest does not experience any water stress during drought periods of the considered simulation period. Empirical evidence of increased forest greenness and sustained evapotranspiration fluxes during prolonged dry periods [e.g., *Huete et al.*, 2006; *Hutyra et al.*, 2007; *Myneni et al.*, 2007; *Saleska et al.*, 2007] provide some support for such an assumption. During calibration, water stress for each tree type was artificially set to zero at each computational step and, consequently, calibration was soil-type and root-distribution independent. As a result, latent heat flux, simulated accounting for the energy constraints (auxiliary material, section S.4, equations (S-10)–(S-12)), essentially represented "potential evapotranspiration."

[33] Note that the total observed daytime sensible and latent heat fluxes are lower than the observed net radiation: by 21.5% during wet season and 19.5% during dry season periods (see a detailed discussion in *Hutyra et al.* [2007]). This substantially complicates the definition of an exact energy partition. Because net radiation was believed to be measured more precisely than heat fluxes, its accurate simulation at the daily and seasonal scales was specifically targeted. The simulated net radiation thus matched observations nearly perfectly, as will be demonstrated in section 3.4.

[34] By design, the model conserves energy and therefore any partition of simulated net radiation into heat fluxes cannot compare favorably with the measured values because of the aforementioned 19.5%–21.5% heat imbalance in observational data. This "surplus" heat energy was distributed among the fluxes of latent, sensible, and ground heat and fluxes going into storage (heat exchanged by precipitation was not accounted for, see *Hutyra et al.* [2007] for further statement of issues related to seasonal heat budget closure). To some extent, the final outcome of calibration is therefore affected by this subjective partition, but it is difficult to assess its exact impact. Several additional simulations were carried out in which parameters were redefined, so as to make either latent or sensible heat receive a higher fraction of the "surplus" energy (not shown). It was inferred that the main conclusions of this study hold, regardless of the decision made in calibration.

[35] Note that the assumption of potential evapotranspiration used in the calibration process aligns well with the concept of water stress avoidance emphasized by the study. The experimental design then allows the exploration of scenarios that can yield fluxes of nearly the same magnitudes as the rates obtained during calibration. The exact implication of assuming the observed fluxes to be potential evapotranspiration is hard to assess; however, a lack of clear water stress signals in the data of *Hutyra et al.* [2007] and the "back-of-the-envelope" estimates implies that the errors cannot be large and affect major inferences of the study.

[36] All of the model parameters used in the description of energy fluxes are provided in Table 2. Among these, the parameters of the "interception" and "water uptake" groups were not modified. Most of the "biophysical" parameters were assigned based on values reported in literature [e.g., *Bonan*, 2008]; only α_{Λ}^{leaf} and τ_{Λ}^{leaf} (visible band) were slightly modified to represent the properties of vegetation acclimation to different vertical positions in the canopy. Using the same considerations, only $V_{max\,25}$ and $\epsilon_{3,4}$ parameters were calibrated in the "biophysical" group.

3.2. Annual Cycle of Evapotranspiration and Water Stress: Identical Root Distributions

[37] The annual cycle of evapotranspiration obtained in the calibration procedure is illustrated in Figure 3a, as the "no stress" scenario, which is qualitatively similar to observations. Figure 3 presents the simulation results as averaged annual cycles of evapotranspiration components computed for the three soil scenarios under the assumption of the *identical* root fractional distribution (i.e., the "control" distribution, see section 2.5.4 and Figure 2b). Specifically, the maximum root depth was set to either Z_{RootD} or $Z_{RootS,}$ and all tree types were assigned to have the identical root profile, which is the control root scenario (see Figure 2b). Under the three soil ("CO," "TH," "MRE") scenarios and the control root scenario, Figure 2b further illustrates that the model exhibits poor performance during dry seasons, i.e., a depressed flux of total evapotranspiration is simulated, as compared to observations (particularly, for the Z_{RootS} scenarios). Evaporation from soil and canopy interception storage shows no sensitivity to any of the soil or root scenarios (Figures 3a and 3b). The poor model

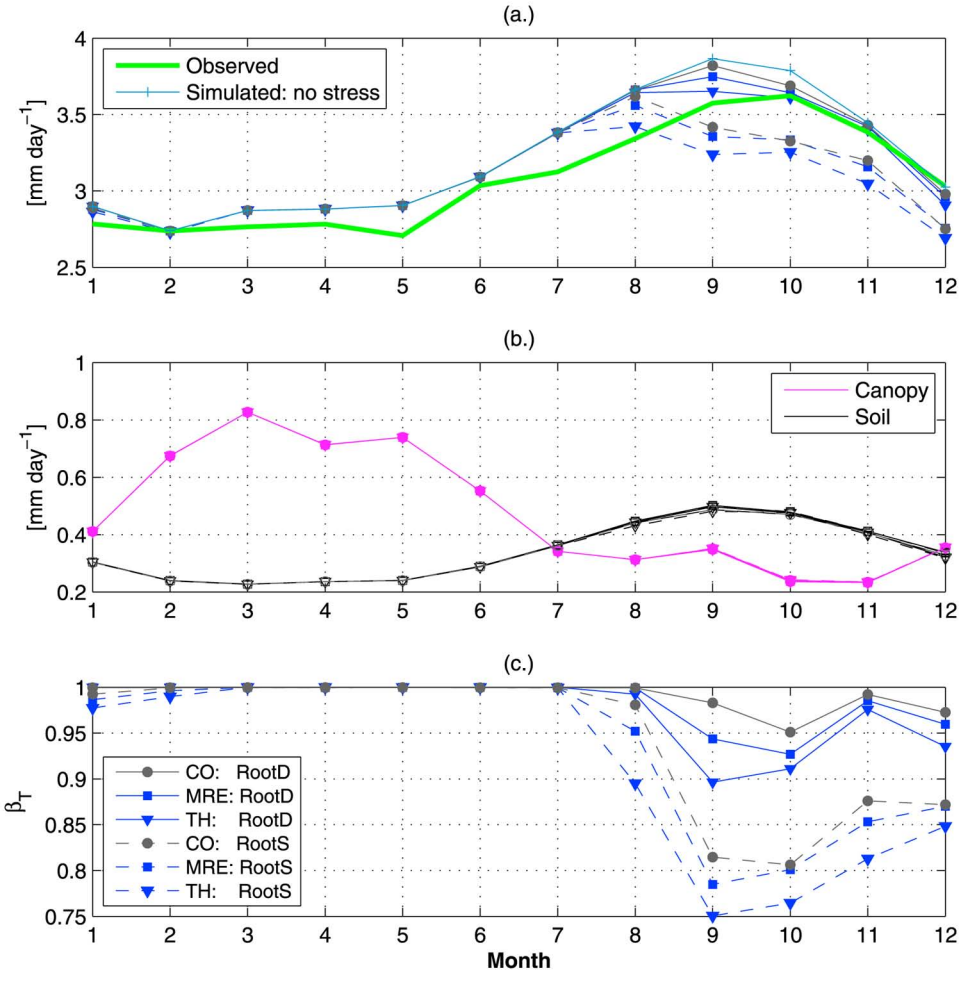

Figure 3. The mean annual cycles of (a) the total evapotranspiration (observed and simulated); (b) evaporation from canopy interception storage and soil surface (simulated); (c) soil moisture availability factor, β_T (Appendix A, equation (A1)), computed as the arithmetic average for the three tree types. The annual cycles were computed for the period of January 2002 to January 2006. The "no stress" scenario (shown in Figure 3a only) corresponds to "potential evapotranspiration," a synthetic case with soil moisture stress set to zero at each computational step (section 3.1). All other scenarios correspond to simulated actual evapotranspiration and exhibit seasonal stress (Figure 3c). "RootD" corresponds to deep roots (the maximum root depth $Z_{\mathrm{RootD}} = 30.2$ m) and the control root scenario (Figure 2b); "RootS" corresponds to shallow roots (the maximum root depth $Z_{\mathrm{RootS}} = 6$ m and the control root scenario. Results for the three soil types are illustrated: "CO," "MRE," and "TH" (Table 1).

performance during August through December period results from a dampening of the transpiration flux as the dry season progresses. The simulations with Z_{RootS} exhibit highest sensitivity for all soil types. Also note that the "no stress" simulation exhibits higher cumulative evapotranspiration than the observed series. This is due to the aforementioned issue of energy imbalance (section 3.1) and the calibration objective to achieve accurate simulation of net radiation at the daily and seasonal scales. The procedure yielded a particular partition of net radiation with simulated evapotranspiration exceeding observed values by ~4.5%.

[38] Figure 3c illustrates the cycles of the soil moisture availability factor (see Appendix A), β_T, computed as the average for the three tree types. The departure of β_T from unity indicates soil control on the transpiration flux and water limitation experienced by vegetation, i.e., $(1 - \beta_T)$ can be interpreted as a metric of water stress. As seen in the figure, all of the soil-root scenarios resulted in some degree of water stress experienced during dry periods. However, the average stress is fairly small for the $Z_{\mathrm{RootD}} = 30.2$ m root scenario. The latter result implies that having (very) deep roots may be a sufficient strategy for avoiding the drought stress; i.e., in this case, the annual root water uptake is distributed over a larger soil depth, providing access to a larger water reservoir and making the uptake density smaller per unit depth.

3.3. Can Niches of Water Uptake Sustain Transpiration?

[39] In addition to the "control" root profile, 12 permutations of individual root profiles were used for the two maximum root depths, Z_{RootD} and Z_{RootS}, resulting in 26 root

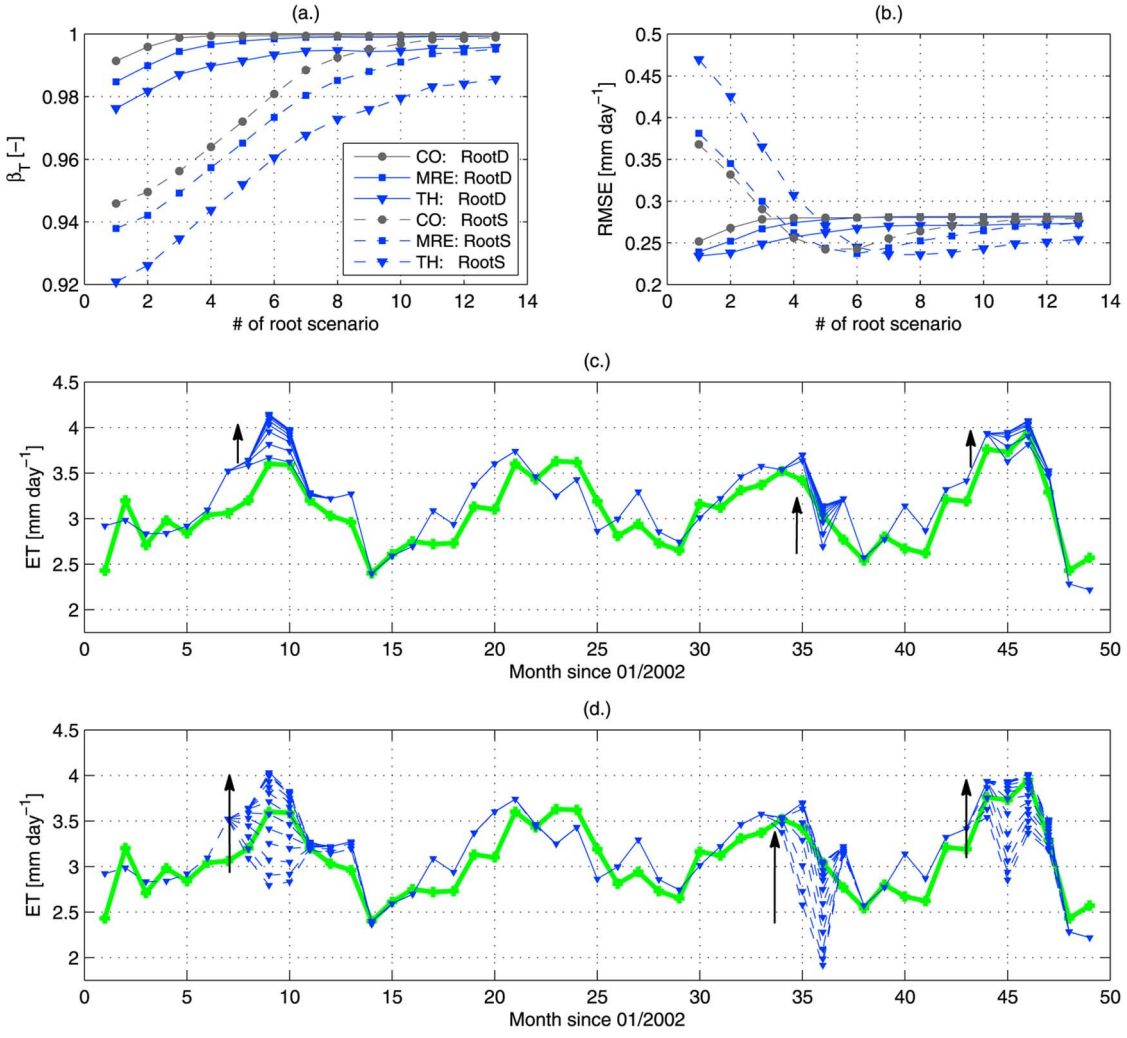

Figure 4. The results of numerical experiments for different scenarios of root distributions. (a) The mean soil moisture availability factor β_T; each point corresponds to a particular permutation scenario of root distributions (section 2.5.4) and was computed as the average value for the three tree types for the simulation period of January 2002 to January 2006. (b) The RMSE of simulated mean daily evapotranspiration (resolved at the monthly scale for dry seasons only); each point corresponds to a particular permutation scenario of root distributions and represents an average value for the simulation period of January 2002 to January 2006. (c) An illustration of the effect of deep root permutation scenarios (the maximum root depth is $Z_{\mathrm{RootD}} = 30.2$ m) on the simulation of daily evapotranspiration resolved at the monthly scale. (d) Same as Figure 4c but with shallower root scenarios (the maximum root depth is $Z_{\mathrm{RootS}} = 6$ m). For Figures 4c and 4d, the arrows indicate a direction of increase of the root scenario number (from 1, the control scenario, to 13, the scenario with distinct root niches; see Figure 2b). The "TH" soil type was used.

scenarios for each soil type (78 scenarios in total). Figure 4a illustrates the factor β_T computed as the time-average value for a particular permutation scenario of root distribution (also averaged across the tree types). As seen, the more vertically "segregated" the profiles become (i.e., the higher the root scenario number), the less overall stress is reproduced by the model. The shallower root depth scenarios exhibit substantially higher sensitivity to root permutations than deeper root depth scenarios. Note that a comparison of absolute magnitudes of evapotranspiration is biased: higher (as compared to observations) latent heat fluxes were simulated intentionally because of the energy imbalance in the observed data (section 3.1).

[40] Figure 4b shows the pattern of the root-mean-square error of mean daily evapotranspiration ($\mathrm{RMSE_{ET}}$) with respect to the observed magnitudes. The behavior of $\mathrm{RMSE_{ET}}$ is not as consistent as that of β_T, i.e., the increase in the root scenario number does not lead to a continuously smaller $\mathrm{RMSE_{ET}}$. This can be explained by the fact that, overall, the model generally overestimates evapotranspiration flux (at maximum, by ~4.5%; section 3.2). The higher β_T implies even larger evapotranspiration magnitudes, which led to a

somewhat poorer comparison of the simulation results in terms of $RMSE_{ET}$ for larger numbers of root scenario.

[41] Figures 4c and 4d interpret the patterns of β_T and $RMSE_{ET}$ behavior with respect to the root scenarios in terms of times series of evapotranspiration flux. The "TH" soil type is used that exhibited the highest water stress for the "control" root profile (Figure 3c) as well as the highest sensitivity of results to the permutations of tree root profiles (Figure 4a). As the root scenario number increases, indicating the growing degree of difference in the root fractional distributions, the simulated water stress during dry seasons vanishes. This is particularly pronounced for the shallower root scenarios (Figure 4d).

[42] As the center of mass of root fractional distribution changes (increasing permutation number), so does the interrelated effect of moisture uptake because of the continuity of the soil water profile. In other words, trees taking up moisture in a particular region of the soil profile necessarily impact uptake and drainage characteristics in other soil layers. The temporal evolution of the soil moisture profile for the two root scenarios corresponding to the maximum root depth Z_{RootS}, the identical, control root scenario and scenario with distinct niches, are shown in Figure 5. Figure 5 clearly shows that the scenario with distinct root niches avoids the extreme seasonal drying of the upper soil layer, where the control root scenario assumes the location of the centers of root mass for all trees. The scenario with distinct root niches leads to a less variable distribution of the drying signal with depth. It can be generally inferred that the variance of soil moisture profile over the root zone depth during dry seasons is smaller for the higher root scenario number (not shown). It can also be concluded that there is no significant effect of root distribution on the soil moisture dynamics during wet periods, except for the year of 2003 that had an unusually low wet season rainfall. By wetting the deep soil profile down to 36 m (not shown), wet season precipitation appears to have a "resetting" effect on soil water in other years. Drying season starts with a fairly uniform profile of moisture near 0.55–0.57 volumetric content.

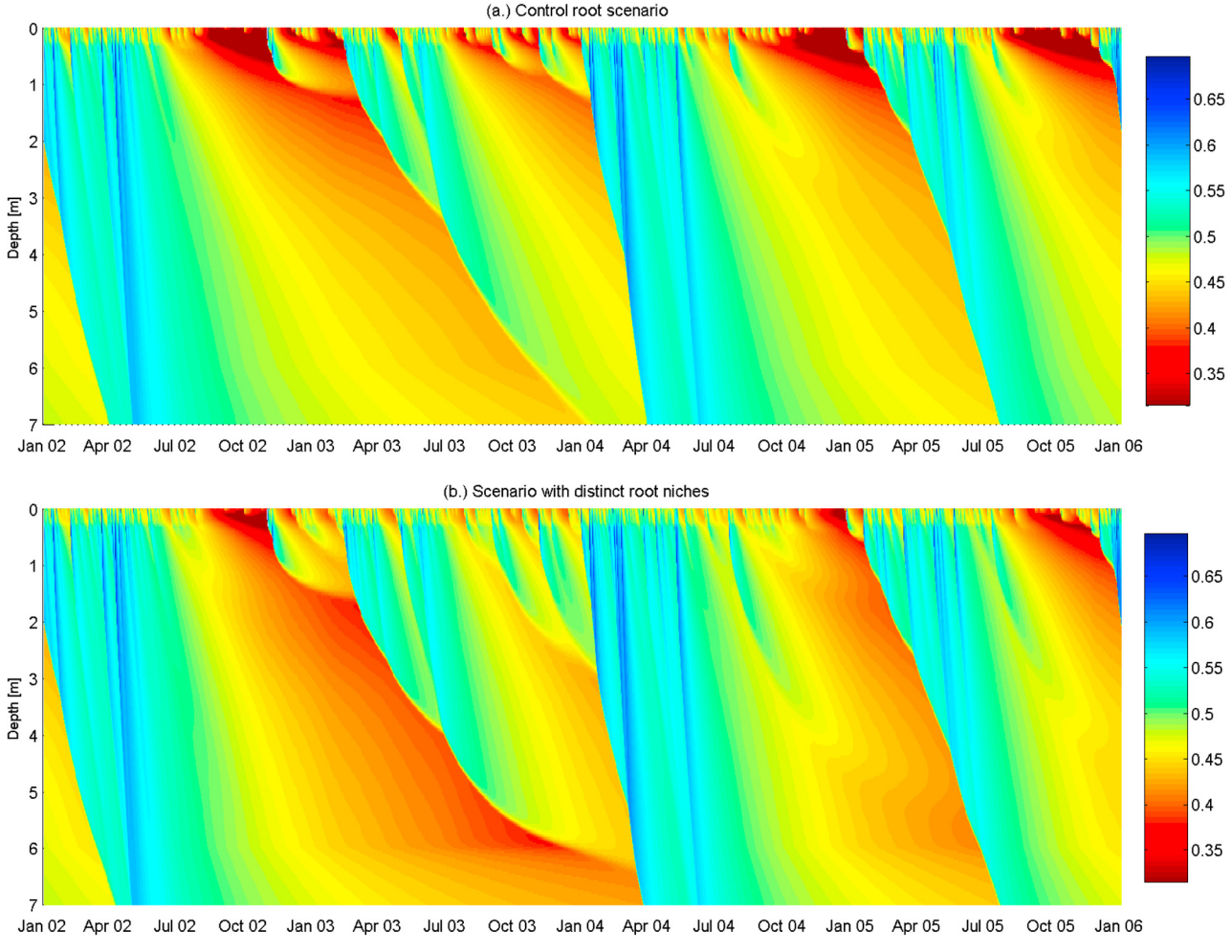

Figure 5. The temporal evolution of soil moisture profile for two root scenarios corresponding to the maximum root depth Z_{RootS}. (a) Simulation results for the control root scenario are illustrated, which exhibits the same fractional distribution of roots for all tree types (Table 3). (b) Simulation results for the scenario with distinct root niches are shown. The scenario assumes that trees of the upper canopy level contain a higher fraction of roots at deeper locations, while trees of the bottom-canopy layer contain higher fraction of roots at shallower soil layers (Table 3). The "CO" soil type was used.

3.4. Seasonality of Energy Fluxes

[43] Figure 6 illustrates the observed and simulated diurnal cycles of energy fluxes. The results correspond to the "CO" soil parameterization, root scenario 6 that did not exhibit appreciable water stress, and thus the results are also representative of calibration (see section 3.1).

[44] The observed cycle of net radiation is almost perfectly reproduced in the simulation results; however, the simulated heat cycles exhibit certain differences from observations. As pointed out in section 3.1, one of the principal difficulties in objective evaluation of such a comparison is the fact that measurements of latent and sensible heat fluxes do not balance the observed net radiation by about 20%. Since the modeled fluxes have to conserve net radiation exactly, the difference with observations was subjectively distributed among the different flux terms. The inclusion of ground heat (small) and storage (auxiliary material, section S.3) terms helps in balancing the net radiative flux, but the overall partition does not appear to be most appropriate. For example, sensible heat flux is generally "overestimated" throughout the day; the latent heat flux is "underestimated" in the first half of the day but is overestimated during the second half. The underestimation effect is partially due to the inclusion of the heat storage term; yet, the net effect is that the total evapotranspiration is somewhat larger than observed, particularly during dry seasons (see Figure 3a). Figures 6c and 6d illustrate that daytime, above-canopy heat fluxes are truly dominated by fluxes associated with vegetation.

[45] The computed temperatures of canopy layers and undercanopy ground (affecting the energy partition shown in Figure 6) are qualitatively consistent (see the auxiliary material, Figure S2): the top-canopy layer exhibits highest temperatures during the daylight hours and the lowest temperatures during nighttime hours; middle- and bottom-canopy layers show progressively smaller diurnal temperature variability and are somewhat warmer than the above-canopy air temperature throughout the day; ground surface temperature has the

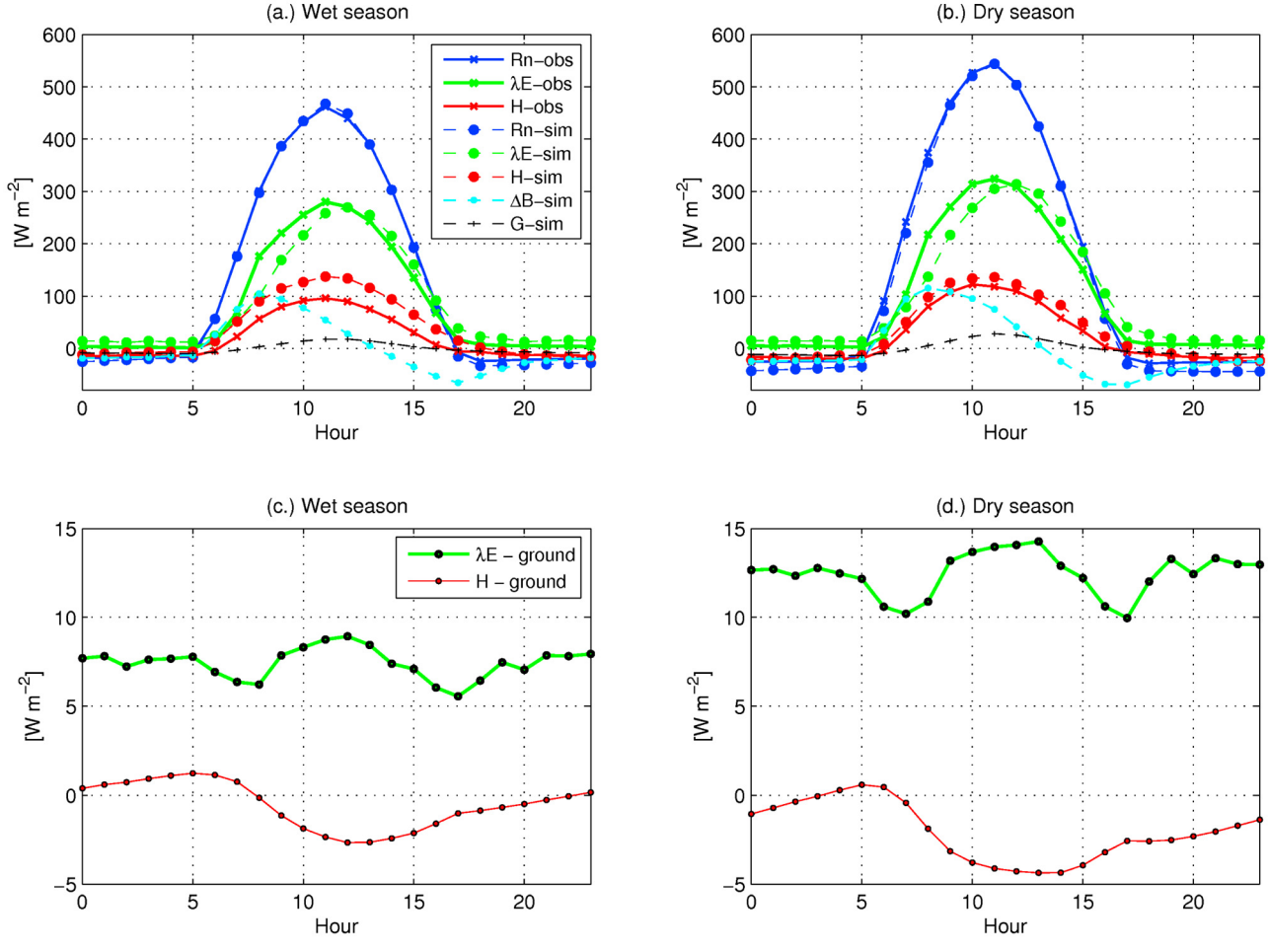

Figure 6. Mean observed and simulated diurnal cycles of energy: (a and c) For wet season (defined as the period between 16 December and 14 July), and (b and d) for dry season (defined as the period between 15 July and 15 December of each calendar year). Notation used: *Rn* is net radiation, λE is latent heat flux, *H* is sensible heat flux, ΔB is change in heat storage in biomass and air, *G* is ground heat flux; "obs" refers to measured series; "sim" refers to simulated results; "ground" refers to contribution from undercanopy ground (simulated cycles only). Simulation results of "CO" soil parameterization (root scenario 6) were used.

lowest diurnal variability and exhibits cooler temperatures during daylight hours because of low levels of radiation reaching the forest floor. The partition of the total-canopy layer latent heat exhibits a peculiar feature of the system: despite the assumed same LAI for all canopy layers, the top-canopy level contributes by far the highest evapotranspiration flux, with lower canopy levels contributing progressively smaller fluxes. Such a feature is apparently related to the substantially higher light levels that are simulated for the top canopy, and, to a lesser extent, to the assigned distribution of V_{max25} values at different levels (Table 2). The implication of this simulation result is that the influence of soil or root distribution on the total forest evapotranspiration should be conveyed through the effect on the function of overstory trees.

3.5. Can Capillary Rise Sustain Transpiration?

[46] Figure 7 illustrates the cumulative upward flux into the root zone of each tree type obtained for the entire simulation period. Only results for the shallower root scenarios are shown, as the fluxes were zero for all soil-root combinations in the case of scenarios corresponding to the maximum root depth Z_{RootD}. The total upward flux is very small for all considered cases and represents smaller than 100th of a percent of the total annual transpiration by trees at all levels. The results are consistent among all soil types. This result is also consistent with *Markewitz et al.* [2010], who focused on soil moisture dynamics at the site of rainfall exclusion experiment [*Nepstad et al.*, 2002].

[47] Note that the simulated subsurface water dynamics may exhibit minor diurnal fluctuations of near-surface soil moisture (not shown). They are related to the capillary effects of periodically developing high gradients of soil water potential during dry periods. Specifically, moisture decreases during daytime because of transpiration and slightly increases at nighttime because of the capillary pull of water from lower depths of higher wetness. These dynamics are more pronounced at shallow soil layers, similar to those shown *da Rocha et al.* [2004 Figure 3], dissipating with depth and becoming insignificant at the root zone bottom of any tree type represented by the model (e.g., Figure 7). Note that the simulated fluctuations are only related to the soil's effect; they have nothing to do with the effect of hydraulic redistribution (not implemented in the model). Yet, the latter mechanism was hypothesized by a number of studies to explain the empirical soil moisture data measured at the km 83 flux tower site of *da Rocha et al.* [2004].

[48] Further, the relevant question one may ask is whether soil hydraulic properties exert a significant effect on the simulated dynamics of evapotranspiration and how they might be related to root vertical variability. One may conjecture, for example, that the "optimal" root distribution would minimize water losses from the root zone. The obtained results only partially corroborate such a statement (the results are only marginally sensitive with respect to the soil type: all used types result in nearly the same flux magnitudes). Specifically, the cumulative net flux from the root zone of overstory trees (obtained for the entire simulation period) exhibits a minimum for the root permutation scenarios 6–8 for Z_{RootD}, and for the scenarios 8–11, in the case of Z_{RootS} (see the auxiliary material, Figure S3). The losses from the root zones of understory trees and mid-canopy trees progressively increase for the deeper root scenarios; in the case of the shallower root scenarios, they reach a minimum for the scenarios 8–11. The modeled leakage is largest for understory and mid-canopy trees for the highest degree of root niche separation. This moisture could be considered a surplus for tall trees; however, one has to take into account the temporal dimension. Specifically, if only wet season leakage increases, there is no benefit for tall trees (they are light limited); if there is an increase in dry season leakage, this is indeed beneficial. Contrasting the notion that only deep roots are sufficient because they have access to a larger moisture reservoir, the moisture surplus can only occur when the uptake density for taller trees becomes smaller in the shallower layers. The corresponding positive effect on deep soil recharge is only obtained when root niche separation assumed.

4. Discussion

4.1. Root Niche Separation as the Likeliest Expression of Adaptation Strategy

[49] Given the amount of water evaporated in the dry season, it is clear that roots must extend to several meters, and existing evidence indicates a depth range of at least 0–18 m [*Davidson et al.*, 2011]. But one cannot unambiguously

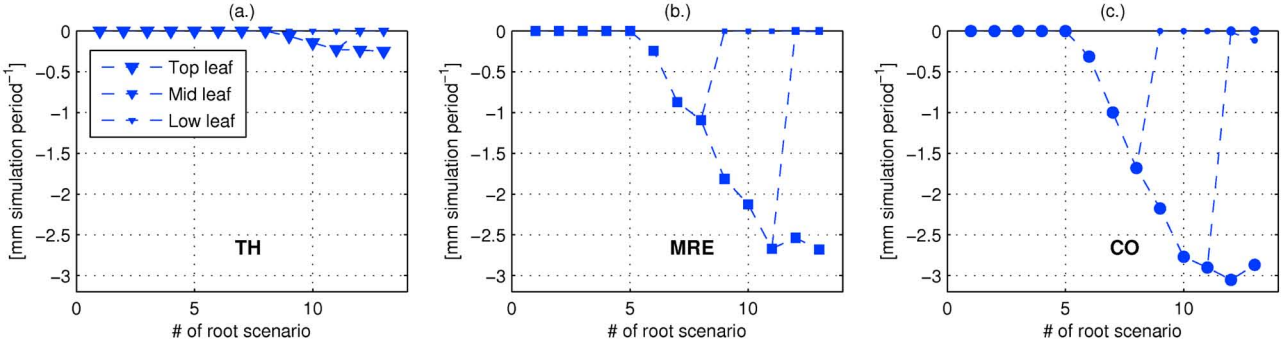

Figure 7. The integrated capillary (upward) flux into the root zone of each tree type over the January 2002 to January 2006 simulation period in relation to the root scenario number. Results correspond to the maximum root depth $Z_{RootS} = 6$ m (the shallower root scenarios). Soil scenarios are denoted in the plots: (a) TH, (b) MRE, and (c) CO. The larger symbol size denotes the higher canopy level.

resolve the exact water-stress avoidance mechanism without additional direct information. This study further argues that existing *indirect* facts point to the plausibility of the root-niche separation hypothesis. The remarkable agreement of outcomes of rainfall exclusion experiments described by *Nepstad et al.* [2002, 2007] and *da Costa et al.* [2010] as well as a pan-tropical assessment of drought-related tree mortality by *Phillips et al.* [2010] and observations for a neotropical forest system by *Condit et al.* [1995] deserve particular consideration.

[50] Specifically, in the long-term rainfall exclusion experiment in Tapajós, detailed by *Nepstad et al.* [2007], a severe, 4-year drought episode was simulated by excluding 60% of throughfall during each wet season from a l-ha forest treatment plot. After 3.2 years of the experiment, "surprisingly, the mortality of large trees began only during the final year of the experiment... the treatment resulted in ... mortality rates increased 4.5-fold among large trees (> 30 cm dbh) and twofold among medium trees (10–30 cm dbh) ... whereas the smallest stems were less responsive" [*Nepstad et al.*, 2007]. The following discussion draws an important analogy between the outcomes of this particular field-monitoring program and inferences of this study.

[51] A priori, if a decrease of wet season precipitation is imposed in numerical simulations, a similar effect of vulnerability of overstory trees should emerge, provided the model realistically reproduces relevant processes of heat-water exchange. Obviously, the effect can only be expressed in terms of increased water stress, not mortality, as the latter cannot be reliably modeled in a deterministic fashion. In an attempt to verify this notion, a synthetic rainfall scenario was developed in which precipitation was reduced by 60% from January through June of each year, over the period of January 2002 to January 2006. The effort intended to mimic the design of *Nepstad et al.* [2002], who carried out their monitoring in close proximity to the km 67 site but over a different period. Figure 8 illustrates a comparison of dynamics of the soil moisture availability factor β_T obtained in simulations with observed and reduced wet season precipitation (see a similar illustration for a different soil type in the auxiliary material, Figure S4). The identical control root scenario and the scenario with distinct root niches (highest differences among the root profiles corresponding to trees at different canopy levels) were used. In simulations described in section 3.3, the control root scenario exhibited a maximum, while the scenario with distinct root niches exhibited minimum water stress, the stress being interpreted as $1 - \beta_T$. As seen in the figure, the latter scenario with observed (not decreased) precipitation forcing exhibits only minor water deficiencies during the three dry seasons, and they are only characteristic of understory trees. Overstory trees are not water limited, and this is the case for both soil types, as inferred from Figure 8.

[52] For the control root scenario, the 60% decrease of wet season precipitation leads to similar water stresses experienced by *all* trees (Figure 8, blue lines) because they have similar moisture conditions in their root profiles. Assuming that moisture sensitivity thresholds of all trees are the same, a similar physiological response to stress conditions would be an outcome. One can further conjecture that there must exist a correlation (albeit uncertain) between the heuristic factor β_T and the probability of mortality, which would imply a nearly uniform mortality rates among all tree size classes than observed in the exclusion experiments. Given the uncertainty of such a correlation and that of mechanistic reasons of tree mortality [e.g., *McDowell et al.*, 2008], the inference is nothing but a "first-order" expectation consistent with water stress hydraulic effects.

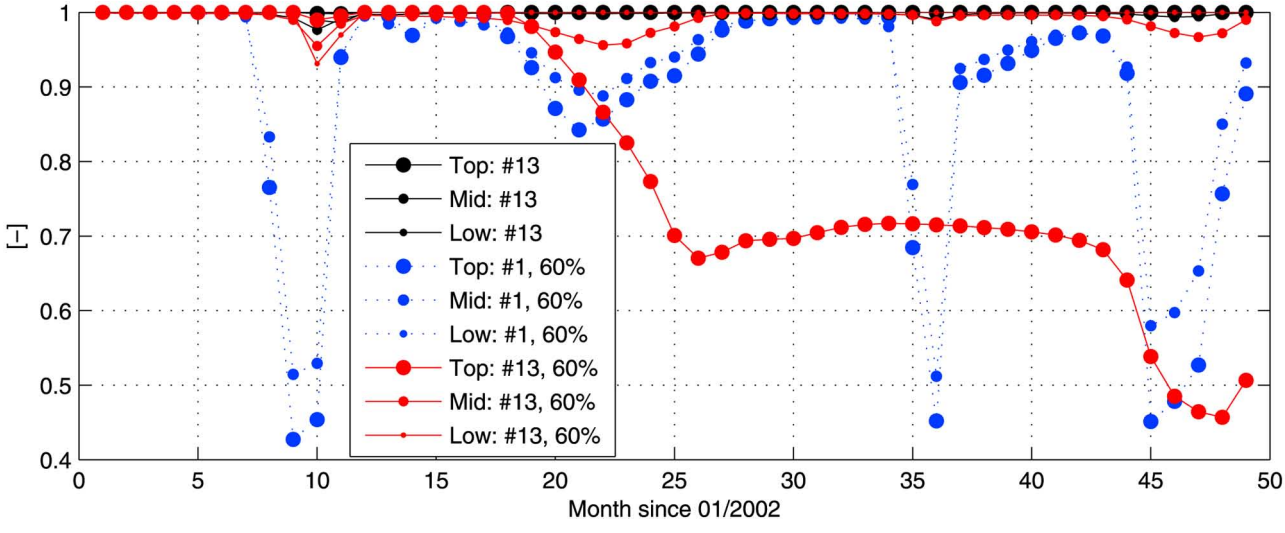

Figure 8. The time series of soil moisture availability factor β_T for each tree type: overstory ("Top") canopy layer, middle ("Mid") canopy layer, and understory ("Low") level canopy over the January 2002 to January 2006 period of simulation. The "CO" soil type was used. The maximum root depth $Z_{\mathrm{RootS}} = 6$ m was used with two types of profile distributions: the control root scenario (the same profile is used for all trees, scenario 1) and the scenario with distinct root niches (scenario 13). The "60%" notation is used for the scenario in which wet season (January through June of each year) precipitation was reduced by 60%.

[53] For the scenario with distinct root niches, the 60% decrease of wet season precipitation does not affect water availability of understory and mid-canopy trees significantly: they are able to transpire most of the dry season and a fraction of wet season precipitation. Similarly, the effect of precipitation shortage is not appreciable for overstory trees until 2–2.5 years after the beginning of simulations. This implies that top-canopy trees exploit water surplus stored in deep soils recharged via earlier wet season rainfall. The water stress sets in toward the end of the second dry season and aggravates severely by the end of the fourth year. At that time, overstory trees cannot satisfy their water needs by more than 50% (Figure 8). Following the above argument of the existence of correlation between the factor β_T and the probability of mortality, in actual conditions, one would expect an increase in mortality of overstory trees. To provide a better insight, Figure 9 provides a graphical illustration of the soil water simulations, when the permutation scenario with distinct root niches is assumed. It shows the depletion of deeper soil moisture reservoir during the first 2–2.5 years. A subsequent aggravation of conditions for depths larger than 3.5 m is apparent, as wetting fronts resulting from rainfall events do not penetrate beyond that depth. The above results demonstrate that under the assumption of equal hydraulic efficiency, root niche separation is a plausible and consistent hypothesis that could explain both the observed robustness in forest productivity during dry seasons as well as vulnerability of canopy-dominant trees to sustained water loss during longer-term droughts.

4.2. What Are the Other Possible Alternative Hypotheses?

[54] Needless to say that this study has explored only a fraction of possible hypotheses that can be drawn for explaining what appears to be a robust drought avoidance strategy by the rainforest. Four alternative explanations closely related to what has been addressed in this study are qualitatively discussed below. Further research is needed to address them in full detail.

[55] Could simply the development of different rooting depths be a sufficient strategy? That is, overstory trees have deep roots, while shorter trees have shallower roots but the centroids of their uptake at *potential rates* overlap, i.e., taller trees do not exhibit a reduced density of moisture uptake in surface layers (for example, see the auxiliary material, Figure S5). Simulations carried out with such a characterizaton of root profiles lead to water stress that is even higher (see the auxiliary material, Figure S6) than that obtained when the control root scenario was used (Figure 8). This result underlines the importance of the uptake density distribution, with a conclusion that screening different depth ranges is insufficient; only deepening of the uptake centroid depth can result in transpiration approaching the potential rates.

[56] Can the "compensation" effect referred to in Appendix A make the above hypothesis of different rooting depths viable? In other words, are there intraseasonal adjustments of centroids of moisture uptake at potential rates or are they seasonally invariant (i.e., determined by the root biomass distribution, as was assumed in this study)?

[57] According to this hypothesis, all trees compete equally for moisture in shallow soil, but as this reservoir is becoming depleted, water uptake shifts deeper in the soil profile, partitioning their uptake throughout the root profile, depending on soil condition. Under this conceptualization, overstory trees with deeper roots would have a larger capacity for adjustments. Given how little is understood about the conditions under which the compensation effects are appropriate to consider and a feasible degree of such a "plasticity" [*Couvreur et al.*, 2012; *Doussan et al.*, 2006; *Javaux et al.*, 2008; *Schneider et al.*, 2010; *van Lier et al.*, 2008], any speculation is quite uncertain. Without getting into a deeper, unsubstantiated discussion, the results of the rainfall exclusion experiment in Tapajós appear to be in qualitative disagreement with such a hypothesis. Specifically, if large trees were competing for shallow soil moisture equally with shorter trees, large trees would exploit shallow soil reservoir to the best they can, satisfying their

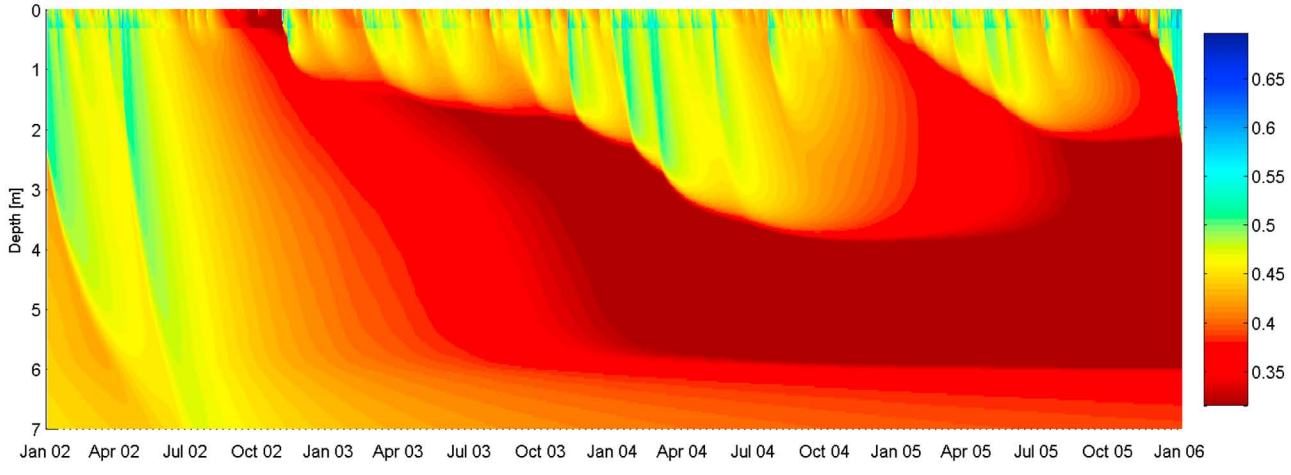

Figure 9. The temporal evolution of soil moisture profile for a scenario in which wet season (January through June of each year) precipitation was reduced by 60%. The simulation results for the scenario with distinct root niches corresponding to the maximum root depth Z_{RootS} are illustrated. The "CO" soil type was used.

high energy inputs. In conditions of the experimental drought, there would be little water left for understory trees within the reach of their shallower root zone. Pronounced signs of stress and an increased mortality would be expected for small trees, while larger trees would thrive. This is directly opposite to what was observed in the Tapajós Forest.

[58] The possibility of the hydraulic redistribution mechanism was previously addressed for this rainforest system from the perspective of a single lumped vegetation layer [*Markewitz et al.*, 2010]. Recently, *Quijano et al.* [2012] employed this mechanism to explore interactions between vegetation species stratified according to their positions within canopy and soil layers for a Mediterranean climate system. Mutualistic dependencies identified in the study of *Quijano et al.* [2012] could possibly play out in the context of differences among rooting profiles hypothesized for the study site. However, direct conjectures are difficult, and further research is needed to determine the plausibility of facilitation of moisture resource use.

[59] Lastly, one cannot fully exclude a dependence of drought tolerance on tree size/age that was not considered in this study. "Vulnerability curves" [*Sperry et al.*, 2002] of taller (and presumbly older) trees can differ from those of younger, shorter trees. Although theoretically feasible, clear evidence supporting such a statement is yet to be presented in research literature.

4.3. Does Root Niche Separation Make Evolutionary Sense?

[60] The biological mechanism of root niche separation is consistent with an adaptive response to the tradeoff between the requirement for sustained productivity for canopy-dominant trees and the risk of sustained soil water limitation from historically infrequent extended droughts in the moist tropics. While the hypothesis appears to be a robust explanation at the system scale, is it consistent with an emergence of evolutionary advantages for an individual?

[61] First, a large tree does need access to larger and buffered storages of soil water to survive droughts, so it needs deep roots. And, in theory, the increased deep root growth can represent an evolved physiological response to breaking into the canopy level (i.e., increase of exposure to light) and a concomitant increase in the aboveground biomass. In this regard, the empirically observed narrow range of root:shoot ratios is not violated. Second, the study argues that while becoming large, a tree needs to reduce its root water uptake in surface layers, where it competes for the same resource with smaller/understory trees. While at a first glance this could be interpreted as an expression of "altruism," it is not so because plant locations are fixed and trees need to adapt not only to climatic environment but also to the "boundary conditions" created by other members of the community; in other words, smaller/understory trees, or, rather, their effects on soil water content, can be considered a part of physical environment of large trees. If such shifts can be indeed assumed, their existence is a response to a long-term condition of mutually unfavorable competition for moisture in surficial layers. Specifically, what emerges from this study is that by growing deeper roots and reducing surficial root uptake, a large tree positively affects the hydrological component of its environment: (1) the downward shift of uptake increases soil moisture in surface layers (2) that leads to a (very) nonlinear growth of soil hydraulic conductivity, and (3) therefore, recharge of deeper soil layers, (4) by reducing the density of uptake in surface layers, a tree compensates the atmospheric demand with a higher uptake at deeper locations. Note that the reduced surficial water uptake can be achieved through (1) a reduction of fine root biomass (i.e., "giving up" this biomass cannot affect the root:shoot ratio appreciably, as coarse roots constitute most of the belowground biomass) or (2) through a possible physiological adjustment of root conductivity in surface layers. Specifically, shallow roots with lower conductivity (which is reasonable to assume through a possibility of tissue suberization or other adaptations) would imply their relatively smaller role for the same biomass. Both of these scenarios were incorporated within the modeling framework indirectly through the functions of relative uptake density. By screening a larger depth and moving the centroid depth of uptake, a large tree effectively separates its uptake niche from that of a shorter tree. Over the evolutionary time, this could represent a stable strategy for trees to survive episodic (but recurrent) droughts, and individuals who failed to create such a separation would fail functionally and therefore evolutionarily.

[62] Lastly, from the perspective of "cost-benefit" analysis, allocation of carbon to deep roots can make evolutionary sense only if this results in a positive carbon increment over a long term. The ability to respond positively to enhanced light conditions during droughts, thereby achieving higher photosynthetic activity and increased CO_2 uptake [e.g., *Goulden et al.*, 2004; *Huete et al.*, 2006; *Hutyra et al.*, 2007; *Myneni et al.*, 2007; *Saleska et al.*, 2007, 2003; *da Rocha et al.*, 2004], would appear to be such a benefit necessarily augmenting any water stress avoidance strategy. A robust increase of carbon assimilation during dry seasons at the study site (for details, see *Hutyra et al.* [2007]) indicates that the two effects could indeed coexist, possibly implying the long-term advantage in terms of costs associated with growth and maintenance of deep roots.

4.4. Wet Season Rainfall as a Key Factor of Ecosystem Stability

[63] Qualitatively comparing Figure 9 with Figure 5, one may propose that by wetting the deep soil profile (down to 36 m, not shown), wet season precipitation has a resetting effect on soil water, so that plants transit to dry season conditions with plentiful moisture. Because overstory trees can access deeper soil layers, moisture that takes its origin from wet season rainfall may exert a buffering effect on severity of drought conditions of any particular year (or two, as the simulations demonstrate). However, if dry conditions persist for a period of time longer than the duration of the buffering effect, overstory trees will reach a "tipping" point in water stress, and a sharply growing mortality would be the outcome. Mid-canopy and understory trees will also likely become vulnerable to drought conditions once the overstory canopy becomes thinner, and a stronger drying effect is exerted on these trees. A further nonlinear effect would be a drier, combustible litter layer in the forest floor [*Ray et al.*, 2005] that would enhance the occurrence of fires and further enhancement of tree mortality [*Cochrane et al.*, 1999]. Consequently, one may conclude that interannual variability of wet season precipitation is an important

characteristic of seasonality that affects stability of the rainforest system at the location of the study site. Currently, global climate models project an increase of dry-season intensity in the eastern and southestern Amazon, while as a reduction of wet-season rainfall appears to be less likely [*Costa and Foley*, 2000; *Malhi et al.*, 2008, 2009]. Serious deficiencies in the structure and resolutions of climate models, however, suggest that the uncertainty of these projections could be very high [*Davidson et al.*, 2012; *Malhi et al.*, 2009]. By missing accurate representation of key atmospheric phenomena, most climate models tend to underestimate current rainfall and, in particular, wet-season precipitation. Relative seasonal changes of rainfall commonly used in climate impact analyses [*Malhi et al.*, 2009] thus could exhibit "dampened" sensitivities.

[64] One may further hypothesize that long-term reduction of wet season precipitation can reach a threshold (see the auxiliary material, section S.6) sufficient to cause complete mortality of overstory trees, defined by inadequate amounts to recharge deep soils for 2–3 years in succession. Although the subsequent transient changes of the forest structure and differential responses of tree species are hard to assess, it is not impossible that the same threshold would represent a tipping point for the entire system, potentially leading to a collapse of the evergreen equatorial biome and its replacement by seasonal forest. This result agrees with the factors limiting the extent of evergreen forests inferred from the biogeographical study of *Hutyra et al.* [2005]. This study found that forests were extant (prior to deforestation) up to a boundary where the accessible soil depth became depleted on average for two or more successive years; i.e., a very different approach led to a similar answer to what was inferred here.

4.5. Robustness of Results

[65] The model uses a number of parameters that are reported in Tables 1 and 2. The ensemble of scenarios of soil hydraulic properties was assumed to include the possible variability of soil textures that occur in the vicinity of the flux tower site [*Hutyra et al.*, 2007]. As the results demonstrate, the essential inferences of the study are not sensitive with respect to a soil hydraulic parameterization.

[66] The parameter space of several vegetation characteristics (section 3.1) has been explored during manual model calibration efforts. However, the parameter values were kept within their narrow "biophysically realistic" ranges that were accepted in numerous previous land-surface modeling studies [e.g., *Bonan*, 2008]. This ensures consistency with field-measured values.

[67] The sensitivity of modeling results was further explored (see the auxiliary material, section S.7) with respect to two parameters that are particularly uncertain and hard to infer from in situ observations. They are the soil water potential at which stomatal closure begins, Ψ^*, and the soil water potential at which plant wilting begins, Ψ_w (Table 2). For lower and higher magnitudes of these parameters, as compared to the values used in all above simulations, the inferences of the study remain the same, as detailed in the auxiliary material, section S.7.

4.6. Potential Applicability to Other Rainforest Areas

[68] One may further investigate the applicability of the root niche separation hypothesis to other sites, where higher mortality of canopy-dominant trees has been observed following drought episodes. For example, *Phillips et al.* [2010] report that large trees are most vulnerable to drought-related mortality, based on an analysis of the response in forest plots to a short, intense drought in the Amazon in 2005. Yet, it is hard to reconcile what appears to be a fairly high sensitivity of tree mortality reported by *Phillips et al.* [2010] study (e.g., increased mortality following a single intense drought) with an apparently more robust forest system in the Tapajós rainfall exclusion experiment, where increased mortality was not observed until the third year, which is about the same time lag necessary for reaching the drought-related tipping point in this modeling study. It may be difficult to draw analogies because the results of *Phillips et al.* [2010] do not allow the evaluation of the circumstances under which mortality occurred at different sites. Such circumstances could include (1) the dynamics of pre-2005 rainfall (i.e., consistently low annual totals could have initiated drought signal buildup in deep soil before the severe 2005 episode; e.g., *Brando et al.* [2008] reported a decrease of wet-season precipitation and an increase of radiation flux for the Amazon Basin over the period of 1996–2005), (2) the increased temperatures and radiation load caused by the real drought (absent from the experimental manipulation), (3) the age characteristics of dying trees (e.g., older trees might be more vulnerable because of imperfections in xylem developed over time), and (4) the differential effects of soil textures. Overall, *Phillips et al.* [2010] data neither strongly confirm nor contradict the hypothesis of root niche separation. More specific, site-level analysis could help identify whether the observation is in agreement/disagreement with the proposed hypothesis.

[69] The main outcomes of the other long-term rainfall exclusion experiment in the Caxiuanã National Forest in the eastern Amazon [*da Costa et al.*, 2010] were very similar to the results of the experiment in Tapajós. Several hydrologically significant differences may be noted for that site: (1) shallower, 10–15 m deep, sandy Oxisol soils; (2) periodic wetting by groundwater at 10–15 m during wet seasons, which most certainly limits the maximum rooting depth, and (3) rainfall was excluded both during dry and wet seasons (although *da Costa et al.* [2010] note that dry seasons in Caxiuanã exhibit higher precipitation than in Tapajós). One may therefore suggest that in the Caxiuanã National Forest: (1) because of a more conductive soil, rainfall more rapidly recharges deeper layers, so large trees may also benefit from dry season rainfall; (2) overstory trees have the opportunity to pull shallower groundwater by capillarity (water table is not affected by rainfall exclusion because of flow advection in the saturated zone), in the case a drought signal develops in soil; and (3) understory-medium trees had somewhat less advantage, as compared to the conditions in Tapajós, because of both experimentally reduced dry season rainfall and more conductive soil. This is consistent with the observation that drought-induced mortality in the Caxiuanã experiment was not as strongly skewed toward large trees as it was in the Tapajós experiment. All of these arguments are consistent with the proposed hypothesis of root niche separation. A more detailed analysis could provide more insight and a stronger possible confirmation, but this is beyond the scope of the current study.

5. Conclusions

[70] This study has addressed linkages between the subsurface moisture dynamics and evapotranspiration of a mature Amazonian rainforest. As in any modeling study, a number of simplifying assumptions were made, which are particularly difficult to avoid for such a complex system as the rainforest. Despite the fairly simple structure, the model mimics essential processes of heat flow and storage with a particular emphasis on soil hydraulics and the effects of tree root distribution on soil moisture dynamics. Specific model assumptions and parameterizations are detailed in the earlier work of *Ivanov et al.* [2008], the auxiliary material (sections S.3 and S.4), and Appendix A.

[71] The study clearly indicates that the soil's capillary action, i.e., the upward unsaturated water flow caused by the gradient in soil matric potential due to transpirational uptake, is not a sufficient mechanism to explain stress avoidance. The conclusion is consistent for all soil types used in the study.

[72] The results indicate that rainforest trees can have at least two or, most likely, a combination thereof, drought avoidance strategies at the study site. First, all trees may have a *very deep* root structure with the majority of roots located in the top soil layer and progressively smaller densities at deeper locations. The open question remains though whether such deep rooting is feasible in terms of plant-soil hydraulics and soil diffusion of oxygen required for root functioning. This study has not addressed this question and detailed/mechanistic models of tree hydraulics and soil processes of gas diffusion would be needed.

[73] The second proposed strategy is that roots of trees located at different canopy levels occupy particular water uptake niches in the soil profile. Specifically, overstory trees receive most radiation and transpire the largest amounts of water; to reduce the risk of vulnerability due to seasonally fluctuating rainfall, these trees developed root systems that are more uniform and extend to larger depths to exploit deeper soil moisture. During drought episodes, fractionally higher root biomass at deeper soil locations (as compared, for example, to the bulk root profile shown in Figure 2a) permits access to moisture originating from wet season precipitation. In contrast, because understory trees are constantly light limited, their relative contribution to the total transpiration flux is significantly smaller as compared to the contribution of overstory trees. They therefore do not need to allocate roots deeply, and their root profiles contain a majority of biomass in shallow surface layers. Full access to water from infrequent dry season precipitation events (and, possibly, a limited access to wet season moisture during drought periods) is sufficient for these trees to avoid seasonal drought stress. Evidence of mortality of large overstory trees by *Nepstad et al.* [2007] at a nearby location in Tapajós and conceptually the same inference from a numerical experiment of reduction of wet season rainfall demonstrated in this study (i.e., the lagged response to drought) confirm that root niche separation is a plausible and consistent expression of the mechanism of drought avoidance strategy at the study location. Furthermore, a remarkable consistency of postdrought mortality of large, canopy-dominant trees across a number of sites including Tapajós, the location of another rainfall exclusion experiment in the eastern Amazon [*da Costa et al.*, 2010], and other tropical areas [*Phillips et al.*, 2010] indicates that differential rooting depth may represent a more geographically widespread mechanism of adaptation of tropical trees to seasonal and interannual drought episodes. The previous biogeographical study of *Hutyra et al.* [2005] also supports the view that recharge of the deep soil reservoir every 2 years, or more often, is sufficient to support evergreen Amazonian forests, but forests do not survive in areas with less-frequent wetting of deep soils.

[74] Whether the hypothesized mechanism is an accurate representation of forest function can be tested with future observations, either of functional response to removal/girdling of large trees or of outcomes of further experiments with rainfall manipulation, or directly, of the size dependence of tree root profiles. For example, if root distributions are independent of tree size, large tree removal should cause a reduction, but no change in the distribution, of soil water removal by roots. The root niche separation hypothesis, by contrast, predicts that large tree removal would cause soil water removal profiles to shift upward. This latter prediction was recently confirmed by observations following selective removal of large trees [*Miller et al.*, 2011] at the km 83 site; this study found a 40% decrease in water withdrawal in the logging gap relative to the intact area and a shift of water withdrawal to shallower locations. Direct observations of size dependence of intact forest tree-root profiles have not previously been possible, but new "barcoding" methods based on matching DNA sequences in belowground roots to aboveground components suggests that direct observational tests may soon become feasible [*Jones et al.*, 2011].

[75] Overall, the proposed biological mechanism of root niche separation is in a conceptual accordance with an adaptive response to the tradeoff between the evolutionary requirement of sustained productivity and the risks imposed by soil water limitation. By mining deep soil moisture, overstory trees exploit the buffering effect of wet season precipitation against severity of drought conditions of any particular year. As explored here in a number of synthetic scenarios, wet season rainfall therefore represents a vital characteristic affecting the stability of the rainforest system at the location of the study site.

Appendix A: Soil Moisture Availability Factor

[76] A heuristic soil moisture availability factor β_T $(-)$ is used to regulate the stomatal conductance based on the soil moisture distribution in the root zone. The formulation is based on a widely used relationship [*Bonan*, 1996; *Feddes et al.*, 2001]:

$$\beta_T = \sum_{j}^{N_{\text{root}}} \beta_{T,j}(z_j)\, r_j(z_j)\,, \tag{A1}$$

$$\beta_{T,j}(z_j) = \max\left[0,\ \min\left(1,\ \frac{\theta_i(z_j) - \theta_w}{\theta^* - \theta_w}\right)\right], \tag{A2}$$

where index j, $j = 1 \ldots N_{\text{root}}$ refers to a depth z_j (m) (zero at the ground surface, positive downward) of the soil profile mesh; the root biomass fraction $r_j(z_j)$ $(-)$ is estimated such that $\sum_j^{N_{\text{root}}} r_j = 1.0$; $\theta(z_j)$ $(\text{m}^3\,\text{m}^{-3})$ is the volumetric soil moisture content; θ_w $(\text{m}^3\,\text{m}^{-3})$ is the moisture content corresponding to the water potential Ψ_w (MPa) at which plant wilting begins (Table 2); and θ^* $(\text{m}^3\,\text{m}^{-3})$ is the threshold moisture content corresponding to the water potential Ψ^* (MPa) at which stomatal closure begins (Table 2). Note that θ_w and θ^* depend on the selected soil water retention parameters (Table 1), following the model of *van Genuchten* [1980].

[77] From equation (A1), the lumped factor $\beta_T \in [0, 1]$ explicitly accounts for soil moisture variability within the root profile by using appropriate weights of root biomass $r_j(z_j)$. Note that the above approach with root-specific densities used as weights to quantify water stress effect is a simplified representation of the uptake function. Plants have been observed to change their active root water uptake zones to meet transpiration needs even when some parts of the root system are water stressed [e.g., *Garrigues et al.*, 2006; *Sharp and Davies*, 1985]. When shallow soil layers (typically containing higher root densities) dry out, plants seem to be capable of shifting water uptake to deeper and moister soil layers to compensate for the decreased root water uptake from shallower layers [*Doussan et al.*, 2006; *Javaux et al.*, 2008; *Schneider et al.*, 2010]. Apparently, such a "compensation" effect cannot be modeled by using the "Feddes-type" approach presented above, and this can be considered a model limitation. However, the degree to which such compensation effects can be expressed is still not well understood, and further research is needed to provide more mechanistic alternatives to the common parameterization equation (A1).

[78] The departure of β_T from unity indicates soil control on the transpiration flux and water limitation; $(1 - \beta_T)$ can thus be interpreted as a metric of water stress experienced by vegetation. Specifically, factors $\beta_{T,j}(z_j)$ are computed at each time step of the energy partition model (hourly) for each individual tree type. The resultant lumped factor β_T is then used to constrain the maximum catalytic capacity of Rubisco $V_{\max}$ [*Ivanov et al.*, 2008, equation (B9)], which in nonlimiting light conditions affects photosynthesis and therefore the stomatal resistance of the plant. Note that the stomatal resistances are computed separately for sunlit ("sun") and shaded ("shd") fractions of each of the canopy layers, $\overline{r}_{s\,i}^{\text{sun}}$ and $r_{s\,i}^{\text{shd}}$ (see *Ivanov et al.* [2008, Appendix B] for details). In total, six dynamic canopy fractions are thus represented in this model implementation. Upscaling of sunlit and shaded fractions to the level of each individual canopy layer is subsequently carried out (auxiliary material, equation (S-6)).

[79] Through their effect on the stomatal resistance, the factors $\beta_{T,j}(z_j)$ affect the estimation of latent heat flux $\lambda E_{v,i}$. Subsequently, factors $\beta_{T,j}(z_j)$ are used as weights for specifying the moisture sinks associated with transpiration in the model of soil water dynamics. Note that $\beta_{T,j}(z_j)$ depends on the soil hydraulic parameterization, the root profile, and the soil water distribution with depth.

[80] **Acknowledgments.** This work was supported by Ziff Postdoctoral Fellowship at the Center for the Environment at Harvard University and partially by the NSF grant 0911444. The technical support of the Center for Advanced Computing at the University of Michigan is acknowledged. Help of Simone Fatichi with data processing is highly appreciated. Insightful comments from three anonymous reviewers have led to substantial improvements of the manuscript material presentation.

References

Baker, I. T., L. Prihodko, A. S. Denning, M. Goulden, S. Miller, and H. R. da Rocha (2008), Seasonal drought stress in the Amazon: Reconciling models and observations, *J. Geophys. Res.*, *113*, G00B01, doi:10.1029/2007JG000644.

Belk, E., D. Markewitz, T. Rassmussen, E. Carvalho, D. Nepstad, and E. Davidson (2007), Modelling the effects of throughfall reduction on soil water content in a Brazilian Oxisol under a moist tropical forest, *Water Resour. Res.*, *43*(14), W08432, doi:10.1029/2006WR005493.

Bohrer, G., G. G. Katul, R. L. Walko, and R. Avissar (2009), Exploring the effects of microscale structural heterogeneity of forest canopies using large-eddy simulations, *Boundary Layer Meteorol.*, *132*, 351–382, doi:10.1007/s10546-009-9404-4.

Bonan, G. (1996), A land surface model (lsm version 1.0) for ecological, hydrological, and atmospheric studies: technical description and user's guide, *Tech. Note TN-417*, NCAR, Boulder, Colo.

Bonan, G. (2008), *Ecological Climatology: Concepts and Applications*, 2nd ed., 568 pp., Cambridge Univ. Press, Cambridge, U. K.

Brando, P., D. Nepstad, E. Davidson, S. Trumbore, D. Ray, and P. Camargo (2008), Drought effects on litterfall, wood production and belowground carbon cycling in an Amazon forest: Results of a throughfall reduction experiment, *Philos. Trans. R. Soc. B*, *363*, 1839–1848.

Brando, P., S. G. A. Baccini, D. Nepstad, P. Beck, and M. C. Christman (2010), Seasonal and interannual variability of climate and vegetation indices across the Amazon, *Proc. Natl. Acad. Sci. U. S. A.*, *107*(33), 14,685–14,690.

Bruno, R., H. D. Rocha, H. D. Freitas, M. Goulden, and S. Miller (2006), Soil moisture dynamics in an eastern Amazonian tropical forest, *Hydrol. Process.*, *20*, 2477–2489.

Caldwell, M., T. Dawson, and J. Richards (1998), Hydraulic lift: Consequences of water efflux from the roots of plants, *Oecologia*, *113*, 151–161.

Cardinot, R. (2008), Efeito de seca experimental sobre a transpiração de uma floresta no centro-leste Amazônico, Ph.D. dissertation, Univ. of Sao Paulo, Brasil.

Cochrane, M., A. Alencar, M. D. Schulze, C. Souza, and D. Nepstad (1999), Positive feedbacks in the fire dynamic of closed canopy tropical forests, *Science*, *284*, 1832–1835.

Collatz, G., J. Ball, C. Grivet, and J. Berry (1991), Physiological and environmental regulation of stomatal conductance, photosynthesis and transpiration—A model that includes a laminar boundary-layer, *Agric. For. Meteorol.*, *52*(2–4), 107–136.

Condit, R., S. P. Hubbell, and R. B. Foster (1995), Mortality rates of 205 neotropical tree and shrub species and the impact of a severe drought, *Ecol. Monogr.*, *65*(4), 419–439.

Costa, M. H., and J. A. Foley (2000), Combined effects of deforestation and doubled atmospheric CO_2 concentrations on the climate of Amazonia, *J. Clim.*, *13*, 18–34.

Couvreur, V., J. Vanderborght, and M. Javaux (2012), A simple three-dimensional macroscopic root water uptake model based on the hydraulic architecture approach, *Hydrol. Earth Syst. Sci.*, Discussions, *9*, 4943–4987.

da Costa, A. C. L., et al. (2010), Effect of 7 yr of experimental drought on vegetation dynamics and biomass storage of an eastern Amazonian rainforest, *New Phytol.*, *187*(3), 579–591.

da Rocha, H., M. Goulden, S. Miller, M. Menton, L. Pinto, H. de Freitas, and A. Figueira (2004), Seasonality of water and heat fluxes over a tropical forest in eastern Amazonia, *Ecol. Appl.*, *14*(4), S22–S32.

Davidson, E., P. A. Lefebvre, P. M. Brando, D. M. Ray, S. E. Trumbore, L. A. Solorzano, J. N. Ferreira, M. M. D. Bustamante, and D. C. Nepstad (2011), Carbon inputs and water uptake in deep soils of an eastern Amazon forest, *For. Sci.*, *57*(1), 51–58.

Davidson, E. A., et al. (2012), The Amazon basin in transition, *Nature*, *481*(7381), 321–332, doi:10.1038/nature10717.

Domingues, T., J. Berry, L. Martinelli, J. Ometto, and J. Ehleringer (2005), Parameterization of canopy structure and leaf-level gas exchange for an eastern Amazonian tropical rain forest (Tapajós National Forest, Para, Brazil), *Earth Interact.*, *9*(17), 1–23.

Doussan, C., A. Pierret, E. Garrigues, and L. Pages (2006), Water uptake by plant roots: II—Modelling of water transfer in the soil root-system with explicit account of flow within the root system-comparison with experiments, *Plant Soil*, *283*(1–2), 99–117.

Eltahir, E. A. B., and R. L. B. Bras (1994), Precipitation recycling in the Amazon Basin, *Q. J. R. Meteorol. Soc.*, *120*(518), 861–880, doi:10.1256/smsqj.51805.

Fan, Y., and G. Miguez-Macho (2010), Potential groundwater contribution to Amazon dry-season evapotransporiration, *Hydrol. Earth Syst. Sci*, *14*, 2039–2056, doi:10.5194/hess-14-2039-2010.

Farquhar, G., S. von Caemmerer, and J. Berry (1980), A biochemical model of photosynthetic CO_2 assimilation in leaves of C-3 species, *Planta*, *149*(1), 78–90.

Fatichi, S., V. Y. Ivanov, and E. Caporali (2012), Investigating interannual variability of precipitation at the global scale: Is there a connection with seasonality?, *J. Clim.*, *25*(16), 5512–5523, doi:10.1175/JCLI-D-11-00356.1.

Feddes, R. A., et al. (2001), Modeling root water uptake in hydrological and climate models, *Bull. Am. Meteorol. Soc.*, *82*(12), 2797–2809.

Garrigues, E., C. Doussan, and A. Pierret (2006), Water uptake by plant roots: I—Formation and propagation of a water extraction front in mature root systems as evidenced by 2D light transmission imaging, *Plant Soil*, *283*(1–2), 83–98.

Goulden, M., S. Miller, H. da Rocha, M. Menton, H. Freitas, A. Figueira, and A. de Sousa (2004), Diel and seasonal patterns of tropical forest CO_2 exchange, *Ecol. Appl.*, *14*(4), S43–S54.

Grant, R., L. Hutyra, R. C. de Oliveira Jr., J. Munger, S. Saleska, and S. Wofsy (2009), Modeling the carbon balance of Amazonian rain forests: Resolving ecological controls on net ecosystem productivity, *Ecol. Monogr.*, *79*, 445–463.

Harris, P., C. Huntingford, and P. M. Cox (2008), Amazon Basin climate under global warming: The role of the sea surface temperature, *Philos. Trans. R. Soc. Ser. B*, *363*, 1753–1759.

Hasler, N., and R. Avissar (2007), What controls evapotranspiration in the Amazon basin?, *J. Hydrometeorol.*, *8*(3), 380–395.

Hou, Z., and Y. Rubin (2005), On minimum relative entropy concepts and prior compatibility issues in vadose zone inverse and forward modeling, *Water Resour. Res.*, *41*, W12425, 13 pp., doi:10.1029/2005WR004082.

Huete, A., K. Didan, E. Shimabukuro, P. Ratana, S. Saleska, L. Hutyra, W. Yang, R. Nemani, and R. Myneni (2006), Amazon rainforests green-up with sunlight in dry season, *Geophys. Res. Lett.*, *33*, L06405, doi:10.1029/2005GL025583.

Huntingford, C., et al. (2008), Towards quantifying uncertainty in predictions of Amazon 'dieback', *Philos. Trans. R. Soc. Ser. B*, *363*, 1857–1864, doi:10.1098/rstb.2007.0028.

Hutyra, L., J. Munger, C. Nobre, S. Saleska, S. Vieira, and S. Wofsy (2005), Climatic variability and vegetation vulnerability in Amazonia, *Geophys. Res. Lett.*, *32*, L24712, doi:10.1029/2005GL024981.

Hutyra, L., J. Munger, S. Saleska, E. Gottlieb, B. Daube, A. Dunn, D. Amaral, P. de Camargo, and S. Wofsy (2007), Seasonal controls on the exchange of carbon and water in an Amazonian rain forest, *J. Geophys. Res.*, *112*, G03008, doi:10.1029/2006JG000365.

Ivanov, V. Y., R. L. Bras, and E. R. Vivoni (2008), Vegetation-hydrology dynamics in complex terrain of semiarid areas: 1. A mechanistic approach to modeling dynamic feedbacks, *Water Resour. Res.*, *44*, W03429, doi:10.1029/2006WR005588.

Javaux, M., T. Schroder, J. Vanderborght, and H. Vereecken (2008), Use of a three-dimensional detailed modeling approach for predicting root water uptake, *Vadose Zone J.*, *7*(3), 1079–1088.

Jipp, P., D. Nepstad, D. Cassel, and C. Carvalho (1998), Deep soil moisture storage and transpiration in forests and pastures of seasonally-dry Amazonia, *Clim. Change*, *39*, 395–412.

Jones, F. A., D. L. Erickson, M. A. Bernal, E. Bermingham, W. J. Kress, E. A. Herre, H. C. Muller-Landau, and B. L. Turner (2011), The roots of diversity: Below ground richness and rooting distributions in a tropical forest revealed by DNA barcodes and inverse modelling, *Plos One*, *6*(9), e24506, doi:10.1371/journal.pone.0024506.

Lee, J., R. S. de Oliveira, T. Dawson, and I. Fung (2005), Root functioning modifies seasonal climate, *Proc. Natl. Acad. Sci. U. S. A.*, *102*(49), 17,576–17,581.

Li, W. H., R. Fu, and R. E. Dickinson (2006), Rainfall and its seasonality over the Amazon in the 21st century as assessed by the coupled models for the IPCC AR4, *J. Geophys. Res.*, *111*, D02111, doi:10.1029/2005JD006355.

Malhi, Y., and J. Wright (2004), Spatial patterns and recent trends in the climate of tropical rainforest regions, *Philos. Trans. R. Soc. London Ser. B*, *359*, 311–329.

Malhi, Y., J. T. Roberts, R. A. Betts, T. J. Killeen, W. Li, and C. A. Nobre (2008), Climate change, deforestation, and the fate of the Amazon, *Science*, *319*, 169–172.

Malhi, Y., L. E. O. C. Aragão, D. Galbraith, C. Huntingford, R. Fisher, P. Zelazowski, S. Sitch, C. McSweeney, and P. Meir (2009), Exploring the likelihood and mechanism of a climate-change-induced dieback of the Amazon rainforest, *Proc. Natl. Acad. Sci. U. S. A.*, *106*(49), 20,610–20,615.

Marengo, J. A. (2004), Interdecadal variability and trends of rainfall across the Amazon basin, *Theor. Appl. Climatol.*, *78*, 79–96, doi:10.1007/s00704-004-0045-8.

Marengo, J. A., C. A. Nobre, J. Tomasella, M. D. Oyama, G. S. de Oliveira, R. de Oliveira, H. Camargo, L. M. Alves, and I. F. Brown (2008), The drought of Amazonia in 2005, *J. Clim.*, *21*, 495–516.

Markewitz, D., S. Devine, E. A. Davidson, P. Brando, and D. C. Nepstad (2010), Soil moisture depletion under simulated drought in the Amazon: Impacts on deep root uptake, *New Phytol.*, *187*(3), 592–607.

McDowell, N., et al. (2008), Mechanisms of plant survival and mortality during drought: Why do some plants survive while others succumb to drought?, *New Phytol.*, *178*(4), 719–739, doi:10.1111/j.1469-8137.2008.02436.x.

Miller, S. D., M. L. Goulden, L. R. Hutyra, M. Keller, S. R. Saleska, S. C. Wofsy, A. M. S. Figueira, H. R. da Rocha, and P. B. de Camargo (2011), Reduced impact logging minimally alters tropical rainforest carbon and energy exchange, *Proc. Natl. Acad. Sci. U. S. A.*, *108*(48), 19431–19435 doi:10.1073/pnas.1105068108.

Myneni, R., et al. (2002), Global products of vegetation leaf area and fraction absorbed par from year one of modis data, *Remote Sens. Environ.*, *83*, 214–231.

Myneni, R., et al. (2007), Large seasonal swings in leaf area of Amazon rainforests, *Proc. Natl. Acad. Sci. U. S. A.*, *104*, 4820–4823.

Nemani, R., C. Keeling, H. Hashimoto, W. Jolly, S. Piper, C. Tucker, R. Myneni, and S. Running (2003), Climate-driven increases in global terrestrial net primary production from 1982 to 1999, *Science*, *300*(5625), 1560–1563.

Nepstad, D., C. de Carvalho, E. Davidson, P. Jipp, P. Lefebvre, G. Negreiro, E. da Silva, T. Stone, S. Trumbore, and S. Vieira (1994), The role of deep roots in the hydrological and carbon cycles of Amazonian forests and pastures, *Nature*, *372*, 666–669.

Nepstad, D., et al. (2002), The effects of partial throughfall exclusion on canopy processes, aboveground production, and biogeochemistry of an Amazon forest, *J. Geophys. Res.*, *107*(D20), 8085, doi:10.1029/2001JD000360.

Nepstad, D., I. Tohver, D. Ray, P. Moutinho, and G. Cardinot (2007), Mortality of large trees and lianas following experimental drought in an Amazon forest, *Ecology*, *88*, 2259–2269.

Neumann, R. B., and Z. G. Cardon (2012), The magnitude of hydraulic redistribution by plant roots: A review and synthesis of empirical and modeling studies, *New Phytol.*, *194*, 337–352, doi:10.1111/j.1469-8137.2012.04088.x.

Nobre, C. A., P. J. Sellers, and J. Shukla (1991), Amazonian deforestation and regional climate change, *J. Clim.*, *4*, 957–988.

Oliveira, R. S., T. E. Dawson, S. S. Burgess, and D. C. Nepstad (2005), Hydraulic redistribution in three Amazonian trees, *Oecologia*, *145*(3), 354–363.

Oyama, M. D., and C. A. Nobre (2003), A new climate-vegetation equilibrium state for Tropical South America, *Geophys. Res. Lett.*, *30*(23), 2199, doi:10.1029/2003GL018600.

Parrota, J., J. K. Francis, and R. Almeida (1995), *Trees of the Tapajós: A Photographic Field Guide*, 371 pp., U.S. Dep. of Agric. For. Serv., Río Piedras, P. R.

Phillips, O. L., et al. (2010), Drought-mortality relationships for tropical forests, *New Phytol.*, *187*(3), 631–646.

Popper, K. (1972), *Objective Knowledge: An Evolutionary Approach*, revised ed., 390 pp., Oxford Univ. Press, New York.

Quijano, J. C., P. Kumar, D. T. Drewry, A. Goldstein, and L. Misson (2012), Competitive and mutualistic dependencies in multispecies vegetation dynamics enabled by hydraulic redistribution, *Water Resour. Res.*, *48*, W05518, doi:10.1029/2011WR011416.

Ray, D., D. Nepstad, and P. Moutinho (2005), Micrometeorological and canopy controls of fire susceptibility in a forested Amazon landscape, *Ecol. Appl.*, *14*, 1664–1678.

Rice, A., E. Hammond, S. Saleska, L. Hutyra, M. Palace, M. Keller, P. de Carmargo, K. Portilho, D. Marques, and S. Wofsy (2004), Carbon balance and vegetation dynamics in an old-growth Amazonian forest, *Ecol. Appl.*, *14*(4), s55–s71.

Romero-Saltos, H., L. Sternberg, M. Moreira, and D. Nepstad (2005), Rainfall exclusion in an eastern Amazonian forest alters soil water movement and depth of water uptake, *Am. J. Bot.*, *92*, 443–455.

Salati, E., and P. B. Vose (1984), Amazon Basin—A system in equilibrium, *Science*, *225*(4658), 129–138, doi:10.1126/science.225.4658.129.

Salazar, L. F., C. A. Nobre, and M. D. Oyama (2007), Climate change consequences on the biome distribution in tropical South America, *Geophys. Res. Lett.*, *34*, L09708, doi:10.1029/2007GL029695.

Saleska, S., et al. (2003), Carbon in Amazon forests: Unexpected seasonal fluxes and disturbance-induced losses, *Science*, *302*, 1554–1557.

Saleska, S., K. Didan, A. Huete, and H. da Rocha (2007), Amazon forests green-up during 2005 drought, *Science*, *318*, 612.

Schlesinger, W. (1997), *Biogeochemistry: An Analysis of Global Change*, 588 pp., Academic, New York.

Schneider, C. L., S. Attinger, J. O. Delfs, and A. Hildebrandt (2010), Implementing small scale processes at the soil-plant interface—The role of root architectures for calculating root water uptake profiles, *Hydrol. Earth Syst. Sci*, *14*(2), 279–289.

Sharp, R. E., and W. Davies (1985), Root-growth and water uptake by maize plants in drying soil, *J. Exp. Bot.*, *36*(170), 1441–1456.

Shuttleworth, W. (1988), Evaporation from Amazonian rainforests, *Proc. R. Soc. London Ser. B*, *233*(1272), 321–346.

Silver, W., J. Neff, M. McGroddy, E. Veldkamp, M. Keller, and R. Cosme (2000), Effects of soil texture on belowground carbon and nutrient storage in a lowland Amazonian forest ecosystem, *Ecosystems*, *3*, 193–209.

Sombroek, W. (2001), Spatial and temporal patterns of Amazon rainfall—Consequences for the planning of agricultural occupation and the protection of primary forests, *Ambio*, *30*(7), 388–396.

Sperry, J. S., U. G. Hacke, R. Oren, and J. P. Comstock (2002), Water deficits and hydraulic limits to leaf water supply, *Plant Cell Environ.*, *25*(2), 251–263.

Taiz, L., and E. Zeiger (2006), *Plant Physiology*, 4th ed., 700 pp., Sinauer Associates, Sunderland, Mass.

Tomasella, J., M. Hodnett, and L. Rossato (2000), Pedotransfer functions for the estimation of soil water retention in Brazilian soils, *Soil Sci. Soc. Am. J.*, *64*, 327–338.

Trenberth, K. E., and T. J. Hoar (1997), El Ninõ and climate change, *Geophys. Res. Lett.*, *24*, 3057–3060.

van Genuchten, M. T. (1980), A closed-form equation for predicting the hydraulic conductivity of unsaturated soils, *Soil Sci. Soc. Am. J.*, *44*, 892–898.

van Lier, Q., J. van Dam, K. Metselaar, R. de Jong, and W. Duijnisveld (2008), Macroscopic root water uptake distribution using a matric flux potential approach, *Vadose Zone J.*, *7*(3), 1065–1078.

Vieira, S., et al. (2004), Forest structure and carbon dynamics in Amazonian tropical rain forests, *Oecologia*, *140*, 468–479.

Werth, D., and R. Avissar (2002), The local and global effects of Amazon deforestation, *J. Geophys. Res.*, *107*D20, 8087, doi:10.1029/2001JD000717.

Werth, D., and R. Avissar (2004), The regional evapotranspiration of the Amazon, *J. Hydrometeorol.*, *5*, 100–109.

Xiao, X., S. Hagen, Q. Zhang, M. Keller, and B. Moore III (2006), Detecting leaf phenology of seasonally moist tropical forests in South America with multi-temporal "MODIS" images, *Remote Sens. Environ.*, *103*(4), 465–473, doi:10.1016/j.rse.2006.04.013.